Joint blind channel shortening and compensation of transmitter I/Q imbalances and CFOs for uplink SC-IFDMA systems

Donatella Darsena[a], Giacinto Gelli[b], Francesco Verde[b]

[a] *Department of Engineering, Parthenope University, Naples I-80143, Italy (e-mail: darsena@uniparthenope.it)*
[b] *Department of Electrical Engineering and Information Technology, University Federico II, Naples I-80125, Italy [e-mail: (gelli, f.verde)@unina.it]*

Abstract

This paper deals with receiver design for the uplink of a single-carrier interleaved frequency-division multiple-access (SC-IFDMA) system, which is a promising candidate for non-adaptive transmission in next-generation wireless systems. In particular, channel shortening is required in asynchronous SC-IFDMA systems operating over highly-dispersive channels, since the length of the cyclic prefix (CP) is insufficient to compensate for the combined effects of timing offsets and channel dispersion; other major sources of performance degradation are the in-phase/quadrature-phase (I/Q) imbalance introduced at each transmitter, and the carrier frequency offsets (CFOs) between the transmitters and the receiver. The proposed multistage receiver is designed to jointly counteract all these impairments: specifically, the minimum mean-output energy (MMOE) criterion is adopted to synthesize a time-domain equalizer, which performs blind multiuser channel shortening of all the user channels (including the corresponding time offsets), without requiring *a priori* knowledge of the channel impulse responses to be shortened, or compensation of the CFOs and transmitter I/Q imbalances. Moreover, after channel shortening and (total or partial) CP removal, the MMOE criterion is also employed to compensate for the CFOs and mitigate I/Q impairments. Monte Carlo computer simulations are carried out to assess the effectiveness of the proposed receiver.

Keywords:
Blind channel shortening, carrier frequency offset (CFO), in-phase/quadrature-phase (I/Q) imbalance, single-carrier interleaved frequency-division multiple-access (SC-IFDMA).

1. Introduction

The choice of the multiple access (MA) scheme for the uplink of a wireless network has a great impact on many system characteristics, such as achievable data rates, spectral and power efficiency, capacity, and implementation complexity of base stations (BSs) and mobile terminals (MTs). The *single-carrier interleaved frequency-division multiple-access* (SC-IFDMA) [1] scheme is a promising solution, which can be derived from orthogonal frequency-division multiple-access (OFDMA) by employing unitary precoding at the transmitter, based on Discrete Fourier Transform (DFT). SC-IFDMA, which can also be regarded as a single-carrier MA scheme that employs block transmission with cyclic prefix (CP), exhibits several advantages, including low envelope fluctuations of the transmit signal, moderate transceiver complexity, high frequency diversity, and good spectral efficiency.

Similarly to OFDMA, various transceiver implementation losses degrade the performance of uplink SC-IFDMA, including *time offsets* (TOs) and *carrier frequency offsets* (CFOs) between the transmitters and the receiver [2, 3], analog front-end *in-phase/quadrature-phase* (I/Q) imbalances [4, 5, 6, 7], and insufficient CP length, that is, the order of the channel impulses responses (CIRs) is larger than the CP length [8]. Such imperfections destroy orthogonality among subcarriers, thus resulting into interblock interference (IBI), intercarrier interference (ICI), and multiple access interference (MAI).

To the best of our knowledge, the challenging problem of jointly counteracting IBI, ICI, and MAI arising from all the previously mentioned losses in the asynchronous OFDMA/SC-IFDMA uplink has not been tackled yet. Indeed, most CFO estimation and compensation techniques [2, 3] for an OFDMA/SC-IFDMA uplink are based on the *quasi-synchronous* (QS) assumption, wherein the CP can perfectly compensate for the combined effects of channel dispersion and TO for each user, and neglect the effects of I/Q front-end impairments. On the other hand, a few solutions [9, 10] deal with joint compensation of CFO and transceiver I/Q imbalances in a QS multicarrier system, but are tailored for a single-user scenario. One noticeable exception is [11], where the CP length is assumed to be smaller than the channel order and a per-tone *time-domain equalizer* (TEQ) is devised, which performs equalization and compensation of CFO and I/Q imbalance. However, the resulting receiver is targeted at a single-user multicarrier system and, most important, the equalization procedure is *not* blind, i.e., a large amount of training is needed to accurately estimate the TEQ parameters.

When the QS assumption is not fulfilled in the uplink, the CP might not be long enough to compensate for channel dispersion plus the residual TOs

of the users; in this case, a multiuser TEQ can be employed at the BS to shorten all the *extended* (i.e., including also the TOs) user CIRs, in order to restore CP properties and ease signal reception. However, existing non-blind [8], [12]-[14] as well as blind [15]-[24] channel-shortening algorithms work only under the assumption of fine frequency synchronization (except for [19]) and perfect I/Q up-conversion/down-conversion. Recently, we have made in [25] a first attempt at designing a multiuser channel shortener in the presence of imperfect frequency synchronization, without nevertheless taking into account I/Q impairments.

In this paper, we consider the uplink of a SC-IFDMA system affected by TOs, CFOs, transmitter I/Q imbalances, and operating over a highly-dispersive channel, where the QS assumption is violated. Since the BS typically performs I/Q demodulation by using high-cost components (e.g., the traditional superheterodyne front-end), we assume that I/Q imbalance at the BS receiver is negligible [4] compared with that at the MTs, which may instead be equipped with cheaper components (e.g., a direct-conversion architecture). In this scenario, we propose an innovative *multistage* BS receiving structure, which orderly performs blind multiuser channel shortening in the time domain (*first stage*), joint multiuser compensation of CFOs and mitigation of transmitter I/Q imbalances (*second stage*), per-user blind matched filtering maximizing the frequency-domain signal-to-noise-ratio (SNR) (*third stage*) and, finally, minimum mean-square error (MMSE) symbol detection for the desired user (*fourth stage*). In particular, we partly rely on the minimum-mean-output-energy (MMOE) channel-shortening approach originally proposed in [20, 22, 23] for a single-user multicarrier system, under the assumptions of perfect time/frequency synchronization and ideal I/Q modulation/demodulation. The receivers developed in [20, 22, 23] have a three-stage structure: the first stage performs linearly-constrained minimization of the mean-output energy of the signal at the output of the channel shortener; such linear constraints are optimally chosen in the second stage so as to maximize the SNR; finally, zero-forcing [20, 22] or maximum-likelihood [23] symbol detection is performed in the last stage.

With respect to [20, 22, 23, 25], our contribution is threefold herein. First, we enlighten that, under certain assumptions, the first stage proposed in [20, 22, 23] achieves blind channel shortening of all the user channels, without requiring knowledge of the extended CIRs to be shortened, or preliminary compensation of the CFOs and I/Q imbalances; however, optimization of the linear constraints has to be carried out *after* performing multiuser CFO compensation and I/Q imbalance mitigation. Second, after (total or partial) CP removal, we additionally employ the MMOE criterion to perform

time-domain compensation of the CFOs and mitigation of the transmitter I/Q imbalances, by exploiting the redundancy present in the SC-IFDMA signals and/or processing the portion (so-called *unconsumed*) of the CP not contaminated by IBI. Third, we show that the proposed design generalizes and subsumes as a special case the receiver proposed in [25], which does not exploit the redundancy contained in the unconsumed portion of the CP and only performs least squares (LS) CFO compensation.

The paper is organized as follows. Section 2 introduces the model for the SC-IFDMA uplink in the presence of TOs, CFOs, and transmitter I/Q imbalances. In Section 3, the proposed receiving structure is designed and discussed. Monte Carlo computer simulation results, aimed at assessing the performance of the proposed receiver, are presented in Section 4, whereas concluding remarks are drawn in Section 5.

Notations: the fields of complex, real, and integer numbers are denoted with $\mathbb{C}$, $\mathbb{R}$, and $\mathbb{Z}$, respectively; matrices [vectors] are denoted with upper [lower] case boldface letters (e.g., $\mathbf{A}$ or $\mathbf{a}$); the field of $m \times n$ complex [real] matrices is denoted as $\mathbb{C}^{m\times n}$ [$\mathbb{R}^{m\times n}$], with $\mathbb{C}^{m}$ [$\mathbb{R}^{m}$] used as a shorthand for $\mathbb{C}^{m\times 1}$ [$\mathbb{R}^{m\times 1}$]; $\{\mathbf{A}\}_{i,j}$ indicates the $(i+1, j+1)$th element of matrix $\mathbf{A} \in \mathbb{C}^{m\times n}$, with $i \in \{0, 1, \ldots, m-1\}$ and $j \in \{0, 1, \ldots, n-1\}$; the superscripts $*$, T, H, -1, and $\dagger$ denote the conjugate, the transpose, the conjugate transpose, the inverse, and the Moore-Penrose generalized inverse of a matrix, respectively; the symbol $\otimes$ denotes Kronecker product of matrices; $\mathbf{0}_m \in \mathbb{R}^m$, $\mathbf{1}_m \in \mathbb{R}^m$, $\mathbf{O}_{m\times n} \in \mathbb{R}^{m\times n}$, and $\mathbf{I}_m \in \mathbb{R}^{m\times m}$ denote the null vector, the vector whose entries are all equal to one, the null matrix, and the identity matrix, respectively; for any $\mathbf{A} \in \mathbb{C}^{m\times n}$, $\|\mathbf{A}\|^2 \triangleq \mathrm{trace}(\mathbf{A}^H\mathbf{A})$ denotes the squared (Frobenius) norm of $\mathbf{A}$; $\mathrm{rank}(\mathbf{A})$ and $\mathrm{trace}(\mathbf{A})$ denote the rank and the trace of $\mathbf{A} \in \mathbb{C}^{m\times n}$; given $\mathbf{A}_0, \mathbf{A}_1, \ldots \mathbf{A}_{n-1} \in \mathbb{C}^{m\times m}$, the matrix $\mathbf{A} = \mathrm{diag}(\mathbf{A}_0, \mathbf{A}_1, \ldots \mathbf{A}_{n-1}) \in \mathbb{C}^{nm\times nm}$ is block diagonal with ith main diagonal block $\mathbf{A}_i$, for $i \in \{0, 1, \ldots, n-1\}$; $j \triangleq \sqrt{-1}$ is the imaginary unit and the operator $\mathbb{E}[\,\cdot\,]$ denotes ensemble averaging.

2. The uplink SC-IFDMA system model

We consider the uplink of SC-IFDMA system [1, 3, 4], wherein $K \leq K_{\mathrm{m}}$ active MTs, with K_{m} denoting the maximum allowable number of users, transmit to a common BS equipped with N_{r} antennas. Each MT is assigned a disjoint set of $M_{\mathrm{u}} \triangleq M/K_{\mathrm{m}}$ subcarriers, where M is the total number of available subcarriers. There are two popular carrier assignment schemes (CASs) for SC-IFDMA systems: subband (the subcarriers allocated to each

user are adjacent) and interleaved (the subcarriers of each user are uniformly spaced over the available bandwidth). In the sequel, we focus on interleaved CAS for two reasons: (i) first of all, unlike subband CAS, interleaved CAS allows fully exploitation of the channel frequency diversity; (ii) in the case of subband CAS, if the CFOs are suitably smaller than the guard intervals, the users' signal can be separated at the BS by means of a bank of digital bandpass filters [2] and, thus, one can resort to single-user channel shortening algorithms, single-user synchronization techniques, and single-user I/Q mitigation methods. Let $i_{k,0} < i_{k,1} < \cdots < i_{k,M_\mathrm{u}-1}$ denote the subcarriers assigned to the kth user, for $k \in \{1, 2, \ldots K\}$, in the case of an interleaved CAS rule, one has $i_{k,\ell} = \ell\, K_\mathrm{m} + \bar{\imath}_k$, for $\ell \in \{0, 1, \ldots, M_\mathrm{u} - 1\}$, where $\bar{\imath}_k \in \{0, 1, \ldots, K_\mathrm{m} - 1\}$ denotes the index of the first subcarrier allocated to the kth user.

At the transmitter, the time-domain symbol sequence of the kth user is parsed into blocks $\mathbf{s}_k(n) \triangleq [s_{k,0}(n), s_{k,1}(n), \ldots, s_{k,M_\mathrm{u}-1}(n)]^T \in \mathbb{C}^{M_\mathrm{u}}$ ($n \in \mathbb{Z}$), which are modeled as circular symmetric complex zero-mean random vectors having correlation matrix $\mathbb{E}[\mathbf{s}_k(n)\, \mathbf{s}_k^H(n)] = \sigma_s^2\, \mathbf{I}_{M_\mathrm{u}}$, with $\mathbf{s}_{k_1}(n_1)$ statistically independent of $\mathbf{s}_{k_2}(n_2)$ for $k_1 \neq k_2$ or $n_1 \neq n_2$. Each block $\mathbf{s}_k(n)$ is first transformed into the frequency domain by DFT, thus obtaining $\widetilde{\mathbf{s}}_k(n) \triangleq \mathbf{W}_\mathrm{dft}\, \mathbf{s}_k(n) \in \mathbb{C}^{M_\mathrm{u}}$, where $\mathbf{W}_\mathrm{dft} \in \mathbb{C}^{M_\mathrm{u} \times M_\mathrm{u}}$ denotes the M_u-point normalized DFT matrix, whose elements are $\{\mathbf{W}_\mathrm{dft}\}_{\ell_1,\ell_2} = M_\mathrm{u}^{-1/2} e^{-j\frac{2\pi}{M_\mathrm{u}}\ell_1\ell_2}$, for $\ell_1, \ell_2 \in \{0, 1, \ldots, M_\mathrm{u} - 1\}$. The resulting block $\widetilde{\mathbf{s}}_k(n)$ is then subject to SC-IFDMA subcarrier mapping, followed by M-point inverse DFT (IDFT) and insertion of a CP of length L_cp. Let $P \triangleq M + L_\mathrm{cp}$, the obtained time-domain block $\mathbf{u}_k(n) \triangleq [u_{k,0}(n), u_{k,1}(n), \ldots, u_{k,P-1}(n)]^T \in \mathbb{C}^P$ can be expressed as

$$\mathbf{u}_k(n) = \mathbf{T}_\mathrm{cp}\, \mathbf{W}_k\, \widetilde{\mathbf{s}}_k(n) \tag{1}$$

where $\mathbf{T}_\mathrm{cp} \triangleq [\mathbf{I}_\mathrm{cp}^T, \mathbf{I}_M]^T \in \mathbb{R}^{P \times M}$ accounts for CP insertion, with $\mathbf{I}_\mathrm{cp} \in \mathbb{R}^{L_\mathrm{cp} \times M}$ gathering the last L_cp rows of $\mathbf{I}_M$, whereas $\mathbf{W}_k \in \mathbb{C}^{M \times M_\mathrm{u}}$ denotes a submatrix of the M-point normalized IDFT matrix, whose (ℓ_1, ℓ_2)th entry is given by $\{\mathbf{W}_k\}_{\ell_1,\ell_2} = M^{-1/2} e^{j\frac{2\pi}{M}\ell_1 i_{k,\ell_2}}$, for $\ell_1 \in \{0, 1, \ldots, M - 1\}$ and $\ell_2 \in \{0, 1, \ldots, M_\mathrm{u} - 1\}$. Vector $\mathbf{u}_k(n)$ undergoes parallel-to-serial conversion, and the resulting sequence $u_k(\ell)$ ($\ell \in \mathbb{Z}$), defined by $u_k(nP + p) = u_{k,p}(n)$ for $p \in \{0, 1, \ldots, P - 1\}$, feeds a digital-to-analog converter operating at rate $1/T_\mathrm{c} = P/T$, where T denotes the symbol length, whose baseband output is up-converted to radio-frequency (RF) by means of a local oscillator.

In RF conversion, it is difficult to achieve a perfect matching of the I and Q branches, especially when cheap components or simple architectures are used [4], [9]-[11]. Following the notation in [4], the impact of such I/Q

imbalance at the kth transmitter can be equivalently described in the baseband model by assuming perfect up-conversion of a distorted version $\widetilde{\mathbf{u}}_k(n)$ of (1), defined by

$$\widetilde{\mathbf{u}}_k(n) \triangleq \alpha_k\, \mathbf{u}_k(n) + \beta_k\, \mathbf{u}_k^*(n) \tag{2}$$

where $\alpha_k \triangleq \cos(\Delta\phi_k) + j\Delta a_k \sin(\Delta\phi_k)$ and $\beta_k \triangleq \Delta a_k \cos(\Delta\phi_k) - j\sin(\Delta\phi_k)$, with Δa_k and $\Delta\phi_k$ denoting the amplitude and phase imbalances of the kth MT, respectively.[1] The ideal case of no transmitter I/Q imbalance corresponds to $\alpha_k = 1$ and $\beta_k = 0$. The degree of imbalance is also measured by using the image-rejection ratio (IRR), which is defined as $\mathrm{IRR}_k \triangleq |\alpha_k|^2/|\beta_k|^2$.

After propagation over a linear time-invariant channel, the continuous-time received signal at each BS antenna is down-converted to baseband and sampled at rate $N_\mathrm{c}/T_\mathrm{c}$, with $N_\mathrm{c} \geq 1$ denoting the oversampling factor. Under the assumption that the I/Q imbalance at the BS is negligible with respect to that of the MTs, let $\mathbf{r}(m) \in \mathbb{C}^Q$ ($m \in \mathbb{Z}$), with $Q \triangleq N_\mathrm{r}\, N_\mathrm{c}$, gather the N_c samples over all the N_r receive antennas in the time interval $[m\, T_\mathrm{c}, (m+1)\, T_\mathrm{c})$, one has

$$\mathbf{r}(m) = \sum_{k=1}^{K} e^{j\frac{2\pi}{M}\epsilon_k m} \sum_{\ell=0}^{L_k+\theta_k} \mathbf{h}_k(\ell)\, [\alpha_k\, u_k(m-\ell) + \beta_k\, u_k^*(m-\ell)] + \mathbf{w}(m) \tag{3}$$

where $\mathbf{h}_k(\ell) \in \mathbb{C}^Q$ gathers the samples of the ℓth tap of the L_k-order finite-impulse response (FIR) channel between the kth MT and the N_r receive antennas of the BS, ϵ_k is the normalized [with respect to the subcarrier spacing $1/(MT_\mathrm{c})$] CFO of the kth user, θ_k denotes the normalized (with respect to the sampling period T_c) TO of the kth user, and $\mathbf{w}(m) \in \mathbb{C}^Q$ accounts for thermal noise.

In the sequel, $\mathbf{w}(m)$ is modeled as a circular symmetric complex zero-mean random vector, with correlation matrix $\mathbb{E}[\mathbf{w}(m)\, \mathbf{w}^H(m)] = \sigma_w^2\, \mathbf{I}_Q$, statistically independent of $u_k(m)$, for $k \in \{1, 2, \ldots K\}$, and with $\mathbf{w}(m_1)$ uncorrelated with $\mathbf{w}(m_2)$ for $m_1 \neq m_2$. Moreover, since each user tries to adjust its uplink synchronization parameters either by exploiting feedback from the BS or relying on synchronization information acquired in downlink, we assume either that the TO θ_k is much smaller than L_k or, in the worst case, it reduces to the two-way propagation delay between the kth user and

[1] For the sake of simplicity, we focus attention on frequency-flat I/Q imbalance; the proposed receiving structure can be generalized to the case of frequency-selective I/Q imbalance with minor modifications.

the BS [2], whereas the CFO ϵ_k is limited to half of the subcarrier spacing, i.e., $|\epsilon_k| < 1/2$.

3. The proposed multistage receiver

Let $L_{\max} \triangleq \max_{k\in\{1,2,\ldots,K\}} \{L_k + \theta_k\}$ denote the maximum channel order (accounting also for the TOs), we assume hereinafter that the CP length is insufficient, i.e., $L_{\max} > L_{\rm cp}$. An insufficient CP length implies that IBI cannot be simply eliminated by means of CP removal: this fact, besides introducing MAI and ICI, prevents the use of conventional frequency synchronization uplink techniques for interleaved CAS [2, 3], which are based on the assumption that IBI is completely eliminated through CP removal. On the other hand, modification of the latter techniques to account for the presence of IBI is mathematically complicated and might lead to computationally burdensome algorithms.

If the CFOs of all the users are not compensated for, after performing DFT and subcarrier demapping, the K users are no more orthogonal, thus increasing the level of MAI in the received signal. Additionally, the presence of transmitter I/Q imbalances, for which the transmitted block $\mathbf{u}_k(n)$ is subject to interference from its complex conjugate version $\mathbf{u}_k^*(n)$, further increases the amount of IBI, ICI, and MAI. To solve these drawbacks, the strategy pursued in this paper consists of performing a preliminary channel-shortening (see Subsection 3.1) by using a TEQ, whose aim is to jointly shorten the extended (i.e., encompassing also the TOs) CIRs of *all* the users in the system, such that their maximum order $L_{\max}$ is cut down to $L_{\rm eff} \leq L_{\rm cp}$: in this case, complete IBI elimination can be obtained by subsequently removing the CP or part thereof.

3.1. First stage: blind multiuser channel shortening

The considered $L_{\rm e}$-order FIR TEQ operates on $L_{\rm e}+1$ consecutive samples of $\mathbf{r}(m)$ in (3), which are gathered in vector $\overline{\mathbf{r}}(m) \triangleq [\mathbf{r}^T(m), \mathbf{r}^T(m-1), \ldots, \mathbf{r}^T(m-L_{\rm e})]^T \in \mathbb{C}^{Q\,(L_{\rm e}+1)}$ given by

$$\overline{\mathbf{r}}(m) = \sum_{k=1}^{K} e^{j\frac{2\pi}{M}\epsilon_k m}\, \mathbf{\Sigma}_k\, \mathbf{H}_k\, [\alpha_k\, \overline{\mathbf{u}}_k(m) + \beta_k\, \overline{\mathbf{u}}_k^*(m)] + \overline{\mathbf{w}}(m) \qquad (4)$$

where $\mathbf{\Sigma}_k \triangleq \mathbf{I}_Q \otimes \mathrm{diag}(1, e^{-j\frac{2\pi}{M}\epsilon_k}, \ldots, e^{-j\frac{2\pi}{M}\epsilon_k L_{\rm e}}) \in \mathbb{C}^{Q\,(L_{\rm e}+1)\times Q\,(L_{\rm e}+1)}$, the channel matrix $\mathbf{H}_k \in \mathbb{C}^{Q(L_{\rm e}+1)\times(L_{\rm g}+1)}$, with $L_{\rm g} \triangleq L_{\rm e}+L_{\max}$, is block Toeplitz having as first Q rows the submatrix $[\mathbf{h}_k(0), \mathbf{h}_k(1), \ldots, \mathbf{h}_k(L_{\max}), \mathbf{0}_Q, \ldots, \mathbf{0}_Q]$,

whereas $\overline{\mathbf{u}}_k(m) \triangleq [u_k(m),\, u_k(m-1), \ldots, u_k(m-L_{\rm g})]^T \in \mathbb{C}^{L_{\rm g}+1}$ and, finally, $\overline{\mathbf{w}}(m) \triangleq [\mathbf{w}^T(m), \mathbf{w}^T(m-1), \ldots, \mathbf{w}^T(m-L_{\rm e})]^T \in \mathbb{C}^{Q\,(L_{\rm e}+1)}$.

To design a blind multiuser channel shortener, we will rely in the following on second-order statistical properties of the received vector $\overline{\mathbf{r}}(m)$. It is easily seen that that $\overline{\mathbf{r}}(m)$ is a zero-mean random vector, whose second-order moments can be expressed in terms of two (possibly time-varying) matrices: the correlation matrix $\mathbf{R}_{\overline{\mathbf{r}}\overline{\mathbf{r}}}(m) \triangleq \mathbb{E}[\overline{\mathbf{r}}(m)\,\overline{\mathbf{r}}^H(m)] \in \mathbb{C}^{Q(L_{\rm e}+1)\times Q(L_{\rm e}+1)}$ and the conjugate correlation matrix $\mathbf{R}_{\overline{\mathbf{r}}\overline{\mathbf{r}}^*}(m) \triangleq \mathbb{E}[\overline{\mathbf{r}}(m)\,\overline{\mathbf{r}}^T(m)] \in \mathbb{C}^{Q(L_{\rm e}+1)\times Q(L_{\rm e}+1)}$. Taking into account that, in the case of interleaved CAS and for[2] $L_{\rm g} < M_{\rm u}$, the zero-mean random vector $\overline{\mathbf{u}}_k(m)$ in (4) turns out to be circular or proper [26], with correlation matrix $\mathbf{R}_{\overline{\mathbf{u}}_k\overline{\mathbf{u}}_k}(m) \triangleq \mathbb{E}[\overline{\mathbf{u}}(m)\,\overline{\mathbf{u}}^H(m)] = \mathbf{R}_{\overline{\mathbf{u}}_k\overline{\mathbf{u}}_k} = \sigma_s^2\,\mathbf{I}_{L_g+1}$, it results that

$$\mathbf{R}_{\overline{\mathbf{r}}\overline{\mathbf{r}}}(m) = \mathbf{R}_{\overline{\mathbf{r}}\overline{\mathbf{r}}} = \sigma_s^2 \sum_{k=1}^{K} (|\alpha_k|^2 + |\beta_k|^2)\,\mathbf{\Sigma}_k\,\mathbf{H}_k\,\mathbf{H}_k^H\,\mathbf{\Sigma}_k^H + \sigma_w^2\,\mathbf{I}_{Q(L_{\rm e}+1)} \tag{5}$$

$$\mathbf{R}_{\overline{\mathbf{r}}\overline{\mathbf{r}}^*}(m) = 2\,\sigma_s^2 \sum_{k=1}^{K} e^{j\frac{4\pi}{M}\epsilon_k m}\,\alpha_k\,\beta_k\,\mathbf{\Sigma}_k\,\mathbf{H}_k\,\mathbf{H}_k^T\,\mathbf{\Sigma}_k^T \tag{6}$$

It can be verified that, when $L_{\rm g} \geq M_{\rm u}$, or for other CASs, such as, e.g., subband CAS [2], the correlation matrix of $\overline{\mathbf{u}}_k(m)$ turns out to be periodically time-varying of period P and singular, thus significantly complicating the design of the channel shortener. Eq. (6) shows that, as a consequence of the transmitter I/Q imbalances (i.e., when $\beta_k \neq 0$), $\mathbf{R}_{\overline{\mathbf{r}}\overline{\mathbf{r}}^*}(m)$ is nonzero and, thus, the vector $\overline{\mathbf{r}}(m)$ turns out to be improper [26]. Moreover, it is apparent from (6) that, due to the presence of the CFOs (i.e., when $\epsilon_k \neq 0$), $\mathbf{R}_{\overline{\mathbf{r}}\overline{\mathbf{r}}^*}(m)$ is time-varying (TV). The improper nature of $\overline{\mathbf{r}}(m)$ suggests that widely-linear (WL) processing [27, 28, 29] of the received data, which jointly elaborates $\overline{\mathbf{r}}(m)$ and its complex conjugate version $\overline{\mathbf{r}}^*(m)$, might improve the channel shortening performances; however, in this case, the resulting TEQ will depend on both $\mathbf{R}_{\overline{\mathbf{r}}\overline{\mathbf{r}}}$ and $\mathbf{R}_{\overline{\mathbf{r}}\overline{\mathbf{r}}^*}(m)$ and, thus, it will be a TV filter, whose blind implementation might be burdensome for large values of K, Q, and $L_{\rm e}$. For such a reason, we focus in the following on a *linear* multiuser channel shortener, whose synthesis, although suboptimal, depends only on $\mathbf{R}_{\overline{\mathbf{r}}\overline{\mathbf{r}}}$ and, hence, turns out to be time-invariant.

The input-output relationship of a linear TEQ is $\mathbf{z}(m) \triangleq \mathbf{F}^H\,\overline{\mathbf{r}}(m)$, where $\mathbf{F} \in \mathbb{C}^{Q(L_{\rm e}+1)\times Q(L_{\rm eff}+1)}$ is a channel-shortening matrix to be de-

[2]The assumption $L_{\rm g} < M_{\rm u}$, which simplifies the TEQ design, limits the number of users to a maximum of $K < M/L_g$.

signed and L_{eff} is a design parameter. Accounting for (4) and defining $\mathbf{d}(m) \triangleq \mathbf{F}^H \overline{\mathbf{w}}(m)$, one has

$$\mathbf{z}(m) = \sum_{k=1}^{K} e^{j\frac{2\pi}{M}\epsilon_k m}\, \mathbf{G}_k^H \left[\alpha_k\, \overline{\mathbf{u}}_k(m) + \beta_k\, \overline{\mathbf{u}}_k^*(m)\right] + \mathbf{d}(m) \tag{7}$$

where $\mathbf{G}_k \triangleq \mathbf{H}_k^H\, \mathbf{\Sigma}_k^H\, \mathbf{F} \in \mathbb{C}^{(L_{\text{g}}+1)\times Q(L_{\text{eff}}+1)}$ denotes the *combined* channel-TEQ matrix of the kth user.

Let $L_{\text{eff}} \leq L_{\text{cp}}$ be a design parameter and $\mathbf{G}_k^H = [\mathbf{G}_{k,\text{left}}^H, \mathbf{G}_{k,\text{right}}^H]$, with $\mathbf{G}_{k,\text{left}} \in \mathbb{C}^{(L_{\text{eff}}+1)\times Q(L_{\text{eff}}+1)}$ and $\mathbf{G}_{k,\text{right}} \in \mathbb{C}^{(L_{\text{g}}-L_{\text{eff}})\times Q(L_{\text{eff}}+1)}$, *perfect* channel shortening amounts to design $\mathbf{F}$ such that $\mathbf{G}_{k,\text{right}} = \mathbf{O}_{(L_{\text{g}}-L_{\text{eff}})\times Q(L_{\text{eff}}+1)}$: in this case, the shortened CIRs of all users are FIR channels of order L_{eff} and the TEQ output (7) becomes

$$\mathbf{z}(m) = \sum_{k=1}^{K} e^{j\frac{2\pi}{M}\epsilon_k m}\, \mathbf{G}_{k,\text{left}}^H \left[\alpha_k\, \overline{\mathbf{u}}_{k,\text{left}}(m) + \beta_k\, \overline{\mathbf{u}}_{k,\text{left}}^*(m)\right] + \mathbf{d}(m) \tag{8}$$

where $\overline{\mathbf{u}}_k(m) = [\overline{\mathbf{u}}_{k,\text{left}}(m)^T, \overline{\mathbf{u}}_{k,\text{right}}(m)^T]^T$, with $\overline{\mathbf{u}}_{k,\text{left}}(m) \in \mathbb{C}^{L_{\text{eff}}+1}$ and $\overline{\mathbf{u}}_{k,\text{right}}(m) \in \mathbb{C}^{L_{\text{g}}-L_{\text{eff}}}$, i.e., only the signal associated with $\mathbf{G}_{k,\text{left}}$ survives in (8).

To blindly enforce the condition $\mathbf{G}_{k,\text{right}} = \mathbf{O}_{(L_{\text{g}}-L_{\text{eff}})\times Q(L_{\text{eff}}+1)}$, we resort to the MMOE approach [20, 23], choosing $\mathbf{F}$ such as to minimize the mean output-energy $\text{MOE}_1(\mathbf{F}) \triangleq \mathbb{E}[\|\mathbf{z}(m)\|^2] = \text{trace}(\mathbf{F}^H \mathbf{R}_{\overline{\mathbf{r}}\overline{\mathbf{r}}}\, \mathbf{F})$ at the TEQ output, with suitable blind constraints aimed at preserving the *desired* signal contribution (associated to $\mathbf{G}_{k,\text{left}}$), which amounts to minimizing the MOE of the *undesired* signal component (associated to $\mathbf{G}_{k,\text{right}}$). The key issue is now to individuate such constraints: in this respect, provided that $L_{\text{eff}} \in \{0, 1, \ldots, \min(L_{\text{e}}, L_{\max})\}$, it can be shown [20] that the $(\delta+1)$th column $\mathbf{h}_{k,\delta}$ of $\mathbf{H}_k$, with $\delta \in \{0, 1, \ldots, L_{\text{eff}}\}$, can be parameterized as $\mathbf{h}_{k,\delta} = \mathbf{\Theta}_\delta\, \boldsymbol{\xi}_{k,\delta}$, where $\mathbf{\Theta}_\delta = [\mathbf{I}_{Q(\delta+1)}, \mathbf{O}_{Q(L_{\text{e}}-\delta)\times Q(\delta+1)}^T]^T \in \mathbb{R}^{Q(L_{\text{e}}+1)\times Q(\delta+1)}$ is a *known* full-column rank matrix, which does not depend on k and satisfies $\mathbf{\Theta}_\delta^T\, \mathbf{\Theta}_\delta = \mathbf{I}_{Q(\delta+1)}$, whereas $\boldsymbol{\xi}_{k,\delta} = [\mathbf{h}_k^T(\delta), \mathbf{h}_k^T(\delta-1), \ldots, \mathbf{h}_k^T(0)]^T \in \mathbb{C}^{Q(\delta+1)}$ gathers samples of the kth CIR to be shortened. Thus, the $(\delta+1)$th column of $\mathbf{\Sigma}_k\, \mathbf{H}_k$, given by $\mathbf{\Sigma}_k\, \mathbf{h}_{k,\delta}$, can be parameterized as

$$\mathbf{\Sigma}_k\, \mathbf{h}_{k,\delta} = \mathbf{\Sigma}_k\, \mathbf{\Theta}_\delta\, \boldsymbol{\xi}_{k,\delta} = \mathbf{\Theta}_\delta\, \overline{\mathbf{\Sigma}}_{k,\delta}\, \boldsymbol{\xi}_{k,\delta} \tag{9}$$

where $\overline{\mathbf{\Sigma}}_{k,\delta} \triangleq \mathbf{I}_Q \otimes \text{diag}(1, e^{-j\frac{2\pi}{M}\epsilon_k}, \ldots, e^{-j\frac{2\pi}{M}\epsilon_k \delta}) \in \mathbb{C}^{Q(\delta+1)\times Q(\delta+1)}$. Moreover, since the recursive relation $\mathbf{\Theta}_{\delta-1} = \mathbf{\Theta}_\delta\, \mathbf{J}_\delta$ holds for $\delta \in \{1, 2, \ldots, L_{\text{eff}}\}$,

where $\mathbf{J}_\delta \triangleq [\mathbf{I}_{Q\delta}, \mathbf{O}_{Q\times Q\delta}^T]^T \in \mathbb{C}^{Q(\delta+1)\times Q\delta}$, the matrix $\mathbf{G}_{k,\text{left}}^H$ is written as

$$\mathbf{G}_{k,\text{left}}^H = \mathbf{F}^H \boldsymbol{\Theta}_{L_\text{eff}} [\mathbf{J}_{L_\text{eff}} \cdots \mathbf{J}_1 \overline{\boldsymbol{\Sigma}}_{k,0} \boldsymbol{\xi}_{k,0}, \mathbf{J}_{L_\text{eff}} \cdots \mathbf{J}_2 \overline{\boldsymbol{\Sigma}}_{k,1} \boldsymbol{\xi}_{k,1}, \ldots, \overline{\boldsymbol{\Sigma}}_{k,L_\text{eff}} \boldsymbol{\xi}_{k,L_\text{eff}}] \tag{10}$$

which shows that the desired contribution can be preserved by imposing the matrix constraint $\mathbf{F}^H \boldsymbol{\Theta}_{L_\text{eff}} = \mathbf{I}_{Q(L_\text{eff}+1)}$. Therefore, the MMOE optimization problem can be expressed as

$$\mathbf{F}_\text{mmoe} = \arg\min_{\mathbf{F}} \text{trace}\left(\mathbf{F}^H \mathbf{R}_{\overline{\mathbf{r}}\overline{\mathbf{r}}} \mathbf{F}\right) \quad \text{subject to} \quad \mathbf{F}^H \boldsymbol{\Theta}_{L_\text{eff}} = \mathbf{I}_{Q(L_\text{eff}+1)} \tag{11}$$

whose solution is given by (see [30])

$$\mathbf{F}_\text{mmoe} = \mathbf{R}_{\overline{\mathbf{r}}\overline{\mathbf{r}}}^{-1} \boldsymbol{\Theta}_{L_\text{eff}} \left(\boldsymbol{\Theta}_{L_\text{eff}}^T \mathbf{R}_{\overline{\mathbf{r}}\overline{\mathbf{r}}}^{-1} \boldsymbol{\Theta}_{L_\text{eff}}\right)^{-1} . \tag{12}$$

The matrix $\mathbf{F}_\text{mmoe}$ can be equivalently rewritten as (see, e.g., [20])

$$\mathbf{F}_\text{mmoe} = \boldsymbol{\Theta}_{L_\text{eff}} - \boldsymbol{\Pi}_1 \left(\boldsymbol{\Pi}_1^T \mathbf{R}_{\overline{\mathbf{r}}\overline{\mathbf{r}}} \boldsymbol{\Pi}_1\right)^{-1} \boldsymbol{\Pi}_1^T \mathbf{R}_{\overline{\mathbf{r}}\overline{\mathbf{r}}} \boldsymbol{\Theta}_{L_\text{eff}} \tag{13}$$

where $\boldsymbol{\Pi}_1 \in \mathbb{R}^{Q(L_\text{e}+1)\times Q(L_\text{e}-L_\text{eff})}$ obeys $\boldsymbol{\Pi}_1^T \boldsymbol{\Theta}_{L_\text{eff}} = \mathbf{O}_{Q(L_\text{e}-L_\text{eff})\times Q(L_\text{eff}+1)}$ and $\boldsymbol{\Pi}_1^T \boldsymbol{\Pi}_1 = \mathbf{I}_{Q(L_\text{e}-L_\text{eff})}$. It is worthwhile to note that $\mathbf{F}_\text{mmoe}$ does not depend on the user index k, and its synthesis needs only knowledge of $\mathbf{R}_{\overline{\mathbf{r}}\overline{\mathbf{r}}}$, which can be consistently estimated from the received data either in batch mode or adaptively [20], without requiring knowledge of the CIRs to be shortened or preliminary compensation of the CFOs and transmitter I/Q imbalances.

The TEQ defined by (12) or (13) satisfies the perfect channel shortening condition $\mathbf{G}_{k,\text{right}} = \mathbf{O}_{(L_\text{g}-L_\text{eff})\times Q(L_\text{eff}+1)}$, $\forall k \in \{1, 2, \ldots, K\}$, in the high-SNR case, i.e., when $\sigma_s^2/\sigma_w^2 \to +\infty$. Indeed, let

$$\mathbf{H} \triangleq [\boldsymbol{\Sigma}_1 \mathbf{H}_1, \boldsymbol{\Sigma}_2 \mathbf{H}_2, \ldots, \boldsymbol{\Sigma}_K \mathbf{H}_K] \in \mathbb{C}^{Q(L_\text{e}+1)\times K(L_\text{g}+1)} \tag{14}$$

$$\mathbf{H}_{k,\text{left}} \triangleq [\mathbf{h}_{k,0}, \mathbf{h}_{k,1}, \ldots, \mathbf{h}_{k,L_\text{eff}}] \in \mathbb{C}^{Q(L_\text{e}+1)\times(L_\text{eff}+1)} \tag{15}$$

$$\mathbf{H}_{k,\text{right}} \triangleq [\mathbf{h}_{k,L_\text{eff}+1}, \mathbf{h}_{k,L_\text{eff}+2}, \ldots, \mathbf{h}_{k,L_\text{g}}] \in \mathbb{C}^{Q(L_\text{e}+1)\times(L_\text{g}-L_\text{eff})} \tag{16}$$

$$\mathbf{H}_\text{right} \triangleq [\boldsymbol{\Sigma}_1 \mathbf{H}_{1,\text{right}}, \boldsymbol{\Sigma}_2 \mathbf{H}_{2,\text{right}}, \ldots, \boldsymbol{\Sigma}_K \mathbf{H}_{K,\text{right}}] \in \mathbb{C}^{Q(L_\text{e}+1)\times K(L_\text{g}-L_\text{eff})} \tag{17}$$

using the limit formula of the Moore-Penrose inverse [31], one has (see also [20, 23])

$$\lim_{\sigma_s^2/\sigma_w^2\to+\infty} \mathbf{G}_k = \begin{bmatrix} \mathbf{H}_{k,\text{left}}^H \boldsymbol{\Sigma}_k^H \boldsymbol{\Theta}_{L_\text{eff}} \\ \mathbf{O}_{(L_\text{g}-L_\text{eff})\times Q(L_\text{eff}+1)} \end{bmatrix} \tag{18}$$

provided that $\mathbf{H}_\text{right}^H \boldsymbol{\Pi}_1$ is full-row rank, which necessarily requires that $Q(L_\text{e} - L_\text{eff}) \geq K(L_\text{g} - L_\text{eff})$. Remembering that $L_\text{g} = L_\text{e} + L_\text{max}$ and

$Q = N_{\rm r}\, N_{\rm c}$, the latter inequality imposes the following upper bound on $L_{\max}$:

$$L_{\max} \leq (L_{\rm e} - L_{\rm eff}) \left(\frac{N_{\rm r}\, N_{\rm c}}{K} - 1 \right) . \tag{19}$$

To achieve IBI suppression through CP removal, the parameter $L_{\rm eff}$ is chosen such that $L_{\rm eff} \leq L_{\rm cp}$. Choosing $L_{\rm eff} < L_{\rm cp}$, perfect IBI suppression is obtained by discarding only the first $L_{\rm eff}$ samples of the CP, i.e., through *partial CP removal*; we will exploit such an option in Subsection 3.2 to gain valuable degrees of freedom in order to jointly compensate the CFOs and the transmitter I/Q imbalances of all the users.

3.2. Second stage: multiuser CFO compensation and I/Q imbalance mitigation

Herein, we assume that the SNR at the BS is sufficiently high; in this case, the TEQ synthesized in Subsection 3.1 assures almost perfect channel shortening, i.e., $\mathbf{G}_{k,\rm right,mmoe} \triangleq \mathbf{H}_{k,\rm right}^H\, \mathbf{\Sigma}_k^H\, \mathbf{F}_{\rm mmoe} \approx \mathbf{O}_{(L_{\rm g}-L_{\rm eff})\times Q(L_{\rm eff}+1)}$, $\forall k \in \{1, 2, \ldots, K\}$; thus, the output vector $\mathbf{z}(m)$ is approximately given by (8), with $\mathbf{G}_{k,\rm left} = \mathbf{G}_{k,\rm left,mmoe} \triangleq \mathbf{H}_{k,\rm left}^H\, \mathbf{\Sigma}_k^H\, \mathbf{F}_{\rm mmoe}$ and $\mathbf{d}(m) = \mathbf{F}_{\rm mmoe}^H\, \overline{\mathbf{w}}(m)$.

After performing polyphase decomposition (with respect to P) of $\mathbf{z}(m)$, removing the first $L_{\rm eff}$ samples of the CP, and collecting the resulting vectors in $\mathbf{Z}(n) \triangleq [\mathbf{z}(nP+L_{\rm eff}), \mathbf{z}(nP+L_{\rm eff}+1), \ldots, \mathbf{z}(nP+P-1)]^T \in \mathbb{C}^{N\times Q(L_{\rm eff}+1)}$, with $N \triangleq P - L_{\rm eff}$, it is shown in Appendix A that[3]

$$\mathbf{Z}(n) = \mathbf{\Psi}\, \mathbf{A}(n) + \mathbf{\Psi}_{\rm mir}\, \mathbf{A}_{\rm mir}(n) + \mathbf{D}(n) \tag{20}$$

where

$$\mathbf{\Psi} \triangleq \sum_{\ell=1}^{K_{\rm m}} \left[\mathbf{\Psi}_1^{(\ell)}, \mathbf{\Psi}_2^{(\ell)}, \ldots, \mathbf{\Psi}_K^{(\ell)} \right] \tag{21}$$

$$\mathbf{\Psi}_{\rm mir} \triangleq \sum_{\ell=1}^{K_{\rm m}} \left[\mathbf{\Psi}_{1,\rm mir}^{(\ell)}, \mathbf{\Psi}_{2,\rm mir}^{(\ell)}, \ldots, \mathbf{\Psi}_{K,\rm mir}^{(\ell)} \right] \tag{22}$$

are $N \times KM_{\rm u}$ complex matrices, with $\mathbf{\Psi}_k^{(\ell)} \in \mathbb{C}^{N\times M_{\rm u}}$ and $\mathbf{\Psi}_{k,\rm mir}^{(\ell)} \in \mathbb{C}^{N\times M_{\rm u}}$ obtained by partitioning $\mathbf{\Psi}_k \triangleq \mathbf{\Omega}_k\, \mathbf{T}_{\rm unc}\, \mathbf{\Delta}_k = [\mathbf{\Psi}_k^{(1)}, \mathbf{\Psi}_k^{(2)}, \ldots, \mathbf{\Psi}_k^{(K_{\rm m})}] \in \mathbb{C}^{N\times M}$ and $\mathbf{\Psi}_{k,\rm mir} \triangleq \mathbf{\Omega}_k\, \mathbf{T}_{\rm unc}\, \mathbf{\Delta}_k^* = [\mathbf{\Psi}_{k,\rm mir}^{(1)}, \mathbf{\Psi}_{k,\rm mir}^{(2)}, \ldots, \mathbf{\Psi}_{k,\rm mir}^{(K_{\rm m})}] \in \mathbb{C}^{N\times M}$,

[3]The subscript "mir" denotes the "mirror" interference created by the I/Q imbalances.

respectively, with

$$\boldsymbol{\Omega}_k \triangleq \mathrm{diag}[1, e^{j\frac{2\pi}{M}\epsilon_k}, \ldots, e^{j\frac{2\pi}{M}\epsilon_k(N-1)}] \tag{23}$$

$$\boldsymbol{\Delta}_k \triangleq K_{\mathrm{m}}^{-1/2}\,\mathrm{diag}[1, e^{j\frac{2\pi}{M}\bar{\iota}_k}, \ldots, e^{j\frac{2\pi}{M}\bar{\iota}_k(M-1)}] \tag{24}$$

complex $N \times N$ matrices, and $\mathbf{T}_{\mathrm{unc}} \triangleq [\mathbf{I}_{\mathrm{unc}}^T, \mathbf{I}_M]^T \in \mathbb{R}^{N\times M}$, with $\mathbf{I}_{\mathrm{unc}} \in \mathbb{R}^{L_{\mathrm{unc}}\times M}$ collecting the last L_{unc} rows of $\mathbf{I}_M$ and $L_{\mathrm{unc}} \triangleq L_{\mathrm{cp}} - L_{\mathrm{eff}}$ denoting the length of the *unconsumed* portion of the CP [32]; moreover, the $KM_{\mathrm{u}} \times Q(L_{\mathrm{eff}}+1)$ complex matrices

$$\mathbf{A}(n) \triangleq \left[\mathbf{A}_1^T(n), \mathbf{A}_2^T(n), \ldots, \mathbf{A}_K^T(n)\right]^T \tag{25}$$

$$\mathbf{A}_{\mathrm{mir}}(n) \triangleq \left[\mathbf{A}_{1,\mathrm{mir}}^T(n), \mathbf{A}_{2,\mathrm{mir}}^T(n), \ldots, \mathbf{A}_{K,\mathrm{mir}}^T(n)\right]^T . \tag{26}$$

are defined in terms of the $M_{\mathrm{u}} \times Q(L_{\mathrm{eff}}+1)$ complex matrices

$$\mathbf{A}_k(n) \triangleq \alpha_k \sqrt{\frac{M}{M_{\mathrm{u}}}} e^{j\frac{2\pi}{M}\epsilon_k(nP+L_{\mathrm{eff}})} \left[\mathbf{1}_{K_{\mathrm{m}}}^T \otimes \boldsymbol{\mathcal{S}}_k(n)\right] \boldsymbol{\Delta}_k^* \boldsymbol{\mathcal{J}} \mathbf{G}_{k,\mathrm{left,mmoe}}^* \tag{27}$$

$$\mathbf{A}_{k,\mathrm{mir}}(n) \triangleq \beta_k \sqrt{\frac{M}{M_{\mathrm{u}}}} e^{j\frac{2\pi}{M}\epsilon_k(nP+L_{\mathrm{eff}})} \left[\mathbf{1}_{K_{\mathrm{m}}}^T \otimes \boldsymbol{\mathcal{S}}_k^*(n)\right] \boldsymbol{\Delta}_k \boldsymbol{\mathcal{J}} \mathbf{G}_{k,\mathrm{left,mmoe}}^* \tag{28}$$

with $\boldsymbol{\mathcal{S}}_k(n) \in \mathbb{C}^{M_{\mathrm{u}}\times M_{\mathrm{u}}}$ be the circulant matrix having the time-domain information block $\mathbf{s}_k(n)$ as first column and $\boldsymbol{\mathcal{J}} \triangleq [\mathbf{I}_{L_{\mathrm{eff}}+1}, \mathbf{O}_{(L_{\mathrm{eff}}+1)\times(M-L_{\mathrm{eff}}-1)}]^T \in \mathbb{R}^{M\times(L_{\mathrm{eff}}+1)}$.

Despite of the inherent complexity of the model, eq. (20) shows the simple fact that, even though IBI has been ideally eliminated, after performing DFT and subcarrier demapping the K users are not yet orthogonal, due to the presence of the CFO-dependent matrix $\boldsymbol{\Psi}$ in (20), which introduces a significant amount of MAI. Moreover, as a consequence of transmitter I/Q imbalances, the block $\boldsymbol{\Psi}\,\mathbf{A}(n)$ is subject to interference from its mirror-image counterpart $\boldsymbol{\Psi}_{\mathrm{mir}}\,\mathbf{A}_{\mathrm{mir}}(n)$. This highlights the need for joint multiuser compensation of CFOs and transmitter I/Q imbalances.

Orthogonality among users can be restored by processing $\mathbf{Z}(n)$ in order to extract an estimate $\widehat{\mathbf{A}}(n)$ of $\mathbf{A}(n)$, which separately gathers the contributions of all the MTs. To this end, we will rely on the second-order statistical properties of matrix $\mathbf{Z}(n)$, under the assumption that the CFOs have been perfectly estimated and, hence, the matrices $\boldsymbol{\Psi}$ and $\boldsymbol{\Psi}_{\mathrm{mir}}$ are exactly known, by deferring to simulations of Section 4 the analysis of the effects of possible CFO estimation errors. It is shown in Appendix B that, due to the combined effects of CFOs and transmitter I/Q imbalances, the conjugate correlation matrix $\mathbf{R}_{\mathbf{Z}\mathbf{Z}^*}(n) \triangleq \mathbb{E}[\mathbf{Z}(n)\,\mathbf{Z}^T(n)] \in \mathbb{C}^{N\times N}$ of $\mathbf{Z}(n)$ is nonzero,

i.e., the random matrix $\mathbf{Z}(n)$ is improper [26] and TV. Therefore, paralleling the discussion made in the synthesis of the channel shortening algorithm, we simplify our design by avoiding to process both $\mathbf{Z}(n)$ and $\mathbf{Z}^*(n)$, choosing thus a simpler (albeit suboptimal) *linear* structure for the estimator of $\mathbf{A}(n)$. Moreover, since the considered modulation is proper, it is also shown in Appendix B that the zero-mean terms $\mathbf{\Psi}\,\mathbf{A}(n)$ and $\mathbf{\Psi}_{\rm mir}\,\mathbf{A}_{\rm mir}(n)$ in (20) are uncorrelated, i.e., $\mathbb{E}[\mathbf{A}(n)\,\mathbf{A}_{\rm mir}^H(n)] = \mathbf{O}_{KM_{\rm u}\times KM_{\rm u}}$, which means that $\mathbf{\Psi}_{\rm mir}\,\mathbf{A}_{\rm mir}(n)$ has to be regarded as a structured disturbance to be suppressed.

To compensate for the CFOs of all the K active users and jointly mitigate their transmitter I/Q imbalances, we employ again a FIR filter $\mathbf{B} \in \mathbb{C}^{KM_{\rm u}\times N}$, which works in cascade with $\mathbf{F}_{\rm mmoe}$, whose input-output relationship is given by

$$\widehat{\mathbf{A}}(n) = \mathbf{B}\,\mathbf{Z}(n) = \mathbf{B}\,\mathbf{\Psi}\,\mathbf{A}(n) + \mathbf{B}\,\mathbf{\Psi}_{\rm mir}\,\mathbf{A}_{\rm mir}(n) + \mathbf{B}\,\mathbf{D}(n)\,. \tag{29}$$

Compensation of the CFOs might be ensured by enforcing the condition $\mathbf{B}\,\mathbf{\Psi} = \mathbf{I}_{KM_{\rm u}\times KM_{\rm u}}$, whereas transmitter I/Q imbalances might be suppressed by imposing the condition $\mathbf{B}\,\mathbf{\Psi}_{\rm mir} = \mathbf{O}_{KM_{\rm u}\times KM_{\rm u}}$; both conditions can be gathered in the linear matrix equation

$$\mathbf{B}\,[\mathbf{\Psi}, \mathbf{\Psi}_{\rm mir}] = [\mathbf{I}_{KM_{\rm u}\times KM_{\rm u}}, \mathbf{O}_{KM_{\rm u}\times KM_{\rm u}}]\,. \tag{30}$$

The matrix equation (30) has a solution if $[\mathbf{\Psi}, \mathbf{\Psi}_{\rm mir}] \in \mathbb{C}^{N\times 2KM_{\rm u}}$ is full-column rank [31], which necessarily requires that $N \geq 2\,K\,M_{\rm u}$; by observing that $N = M + L_{\rm unc}$, with $L_{\rm unc} \ll M$, and $M_{\rm u} = M/K_{\rm m}$, it follows that a necessary condition is $K \lessapprox K_{\rm m}/2$, i.e., the system can work half-load at most, which is an overly restrictive condition on the number of MTs.

To relax such a constraint on the maximum number of users, we pursue a different approach, by observing that the full-column rank property of $[\mathbf{\Psi}, \mathbf{\Psi}_{\rm mir}]$ is a sufficient but not necessary condition for achieving joint CFO compensation and transmitter I/Q imbalance mitigation. Indeed, the linear matrix equation $\mathbf{B}\,\mathbf{\Psi} = \mathbf{I}_{KM_{\rm u}\times KM_{\rm u}}$ is consistent (i.e., it admits at least one solution) if $\mathbf{\Psi}$ is full-column rank,[4] that is, $N \geq K\,M_{\rm u}$ and $\mathrm{rank}(\mathbf{\Psi}) = 2\,K\,M_{\rm u}$: in this case, the solution of $\mathbf{B}\,\mathbf{\Psi} = \mathbf{I}_{KM_{\rm u}\times KM_{\rm u}}$ is *not* unique [31] and, thus, we propose to exploit the remaining free parameters in $\mathbf{B}$ to mitigate the effects of the transmitter I/Q imbalances. Towards this aim, the matrix $\mathbf{B}$ is chosen here so as to minimize the MOE at the output of the

[4]Provided that $N \geq K\,M_{\rm u}$, it can be proven (details are omitted) that $\mathbf{\Psi}$ is always full-column rank if $|\epsilon_{k_1} - \epsilon_{k_2}| < 1$, for any $k_1 \neq k_2 \in \{1, 2, \ldots, K\}$.

FIR filter, which is given by $\mathrm{MOE}_2(\mathbf{B}) \triangleq \mathbb{E}[\|\mathbf{B}\,\mathbf{Z}(n)\|^2] = \mathrm{trace}(\mathbf{B}\,\mathbf{R}_{\mathbf{ZZ}}\,\mathbf{B}^H)$, where $\mathbf{R}_{\mathbf{ZZ}} \triangleq \mathbb{E}[\mathbf{Z}(n)\,\mathbf{Z}^H(n)] \in \mathbb{C}^{N\times N}$ is the correlation matrix of $\mathbf{Z}(n)$, whose explicit expression has been calculated in Appendix B. Therefore, joint CFO compensation and mitigation of the transmitter I/Q imbalances amounts to choosing $\mathbf{B}$ as the solution of the following MMOE problem

$$\mathbf{B}_{\mathrm{mmoe}} = \arg\min_{\mathbf{B}} \mathrm{trace}(\mathbf{B}\,\mathbf{R}_{\mathbf{ZZ}}\,\mathbf{B}^H) \quad \text{subject to } \mathbf{B}\,\mathbf{\Psi} = \mathbf{I}_{KM_{\mathrm{u}}\times KM_{\mathrm{u}}} \tag{31}$$

whose solution is given by (see, e.g., [30])

$$\mathbf{B}_{\mathrm{mmoe}} = \left(\mathbf{\Psi}^H\,\mathbf{R}_{\mathbf{ZZ}}^{-1}\,\mathbf{\Psi}\right)^{-1}\mathbf{\Psi}^H\,\mathbf{R}_{\mathbf{ZZ}}^{-1}\,. \tag{32}$$

The matrix $\mathbf{B}_{\mathrm{mmoe}}$ can be equivalently rewritten as (see, e.g., [20])

$$\mathbf{B}_{\mathrm{mmoe}} = \mathbf{\Psi}^{\dagger} - \boldsymbol{\mathcal{B}}_{\mathrm{mmoe}}\,\mathbf{\Pi}_2 = \mathbf{B}_{\mathrm{mmoe}}^{(f)} - \mathbf{B}_{\mathrm{mmoe}}^{(a)} \tag{33}$$

with $\boldsymbol{\mathcal{B}}_{\mathrm{mmoe}} \triangleq \mathbf{B}_{\mathrm{mmoe}}^{(f)}\,\mathbf{R}_{\mathbf{ZZ}}\,\mathbf{\Pi}_2^H(\mathbf{\Pi}_2\,\mathbf{R}_{\mathbf{ZZ}}\,\mathbf{\Pi}_2^H)^{-1}$, where the fixed term $\mathbf{B}_{\mathrm{mmoe}}^{(f)}$ represents the minimum-norm (in the Frobenius sense) solution of the constraint in (31), whereas $\mathbf{\Pi}_2 \in \mathbb{C}^{(N-KM_{\mathrm{u}})\times N}$ is the *signal blocking matrix*, satisfying $\mathbf{\Pi}_2\,\mathbf{\Psi} = \mathbf{O}_{(N-KM_{\mathrm{u}})\times KM_{\mathrm{u}}}$ and $\mathbf{\Pi}_2\,\mathbf{\Pi}_2^T = \mathbf{I}_{N-KM_{\mathrm{u}}}$. Observe that $\mathbf{B}_{\mathrm{mmoe}}$ does not depend on the user index k, and its synthesis needs only the knowledge of $\mathbf{R}_{\mathbf{ZZ}}$, which can be consistently estimated from the received data either in batch mode or adaptively [23], without requiring knowledge of I/Q imbalance parameters. Moreover, it is worth noting that, if the unconsumed part of CP is zeroed, i.e., $L_{\mathrm{unc}} = 0$ implying $N = M$, *and* all users in the SC-IFDMA system are active, that is, $K = K_{\mathrm{m}}$ implying $KM_{\mathrm{u}} = M$, then the adaptive part $\mathbf{B}_{\mathrm{mmoe}}^{(a)}$ of the MMOE equalizer vanishes and $\mathbf{B}_{\mathrm{mmoe}}$ reduces to its fixed part $\mathbf{B}_{\mathrm{mmoe}}^{(f)} = \mathbf{\Psi}^{\dagger}$: in this case, only CFO compensation is performed in this stage and the proposed MMOE-based second stage boils down to the LS-based second stage developed in [25]. Therefore, if the system works at full load, i.e., $K = K_{\mathrm{m}}$, partial CP removal, i.e., $L_{\mathrm{unc}} > 0$, is mandatory for achieving satisfactory I/Q imbalance mitigation in the case of non-negligible CFOs. On the other hand, when $K < K_{\mathrm{m}}$, that is, the system is not at full load, mitigation of I/Q imbalances in this stage can be achieved even when $L_{\mathrm{unc}} = 0$ (total CP removal).

3.3. Third stage: per-user blind matched filtering

Assuming that IBI has been suppressed, CFOs have been perfectly compensated, and MAI due to I/Q imbalances has been mitigated, we perform a per-user blind matched filtering, aimed at maximizing the SNR at the

input of the fourth stage. Let $\boldsymbol{\gamma} \in \mathbb{C}^{Q(L_{\text{eff}}+1)}$ denotes the weight vector of the matched filter, taking into account (29) and exploiting the constraint $\mathbf{B}_{\text{mmoe}}\,\boldsymbol{\Psi} = \mathbf{I}_{KM_{\text{u}}\times KM_{\text{u}}}$, the filter output $\mathbf{x}(n) \in \mathbb{C}^{KM_{\text{u}}}$ can be approximatively expressed as

$$\mathbf{x}(n) \triangleq \widehat{\mathbf{A}}(n)\,\boldsymbol{\gamma} = [\mathbf{A}(n) + \mathbf{B}_{\text{mmoe}}\,\mathbf{D}(n)]\,\boldsymbol{\gamma} \tag{34}$$

where we have assumed that $\mathbf{B}_{\text{mmoe}}\,\boldsymbol{\Psi}_{\text{mir}} \approx \mathbf{O}_{(KM_{\text{u}})\times(KM_{\text{u}})}$, i.e., the MAI contribution due to transmitter I/Q impairments is almost negligible. Let $\mathbf{R}_k \triangleq [\mathbf{O}_{(k-1)M_{\text{u}}\times M_{\text{u}}}, \mathbf{I}_{M_{\text{u}}}, \mathbf{O}_{(K-k)M_{\text{u}}\times M_{\text{u}}}] \in \mathbb{R}^{M_{\text{u}}\times KM_{\text{u}}}$ represent the matrix picking out the M_{u}-dimensional sub-vector of $\mathbf{x}(n)$ corresponding to the kth user, after having performed the M_{u}-point DFT, the resulting kth user data vector can be expressed as

$$\begin{aligned}\mathbf{q}_k(n) \triangleq \mathbf{W}_{\text{dft}}\,\mathbf{R}_k\,\mathbf{x}(n) = \mathbf{Q}_k(n)\,\boldsymbol{\gamma} = \alpha_k\sqrt{\frac{M}{M_{\text{u}}}}\,e^{j\frac{2\pi}{M}\epsilon_k(nP+L_{\text{eff}})}\\ \times \mathbf{W}_{\text{dft}}\,\left[\mathbf{1}_{K_{\text{m}}}^T \otimes \boldsymbol{\mathcal{S}}_k(n)\right]\,\boldsymbol{\Delta}_k^*\,\boldsymbol{\mathcal{J}}\,\mathbf{G}_{k,\text{left,mmoe}}^*\,\boldsymbol{\gamma}\\ + \mathbf{W}_{\text{dft}}\,\mathbf{R}_k\,\mathbf{B}_{\text{mmoe}}\,\mathbf{D}(n)\,\boldsymbol{\gamma}\end{aligned} \tag{35}$$

with $\mathbf{Q}_k(n) \triangleq \mathbf{W}_{\text{dft}}\mathbf{R}_k\widehat{\mathbf{A}}(n) \in \mathbb{C}^{M_{\text{u}}\times Q(L_{\text{eff}}+1)}$. Remembering that $\boldsymbol{\mathcal{S}}_k(n)$ is the circulant matrix having the time-domain information block $\mathbf{s}_k(n)$ as first column, by using eigenstructure properties of circulant matrices, the kth user data-vector (35) can be rewritten as

$$\begin{aligned}\mathbf{q}_k(n) = \alpha_k\sqrt{M}e^{j\frac{2\pi}{M}\epsilon_k(nP+L_{\text{eff}})}\,\widetilde{\mathbf{S}}_k(n)\,\mathbf{W}_{\text{dft}}\,\boldsymbol{\Delta}_{k,\text{sub}}^*\,\boldsymbol{\mathcal{J}}_{\text{sub}}\,\mathbf{G}_{k,\text{left,mmoe}}^*\,\boldsymbol{\gamma}\\ + \mathbf{W}_{\text{dft}}\,\mathbf{R}_k\,\mathbf{B}_{\text{mmoe}}\,\mathbf{D}(n)\boldsymbol{\gamma}\end{aligned} \tag{36}$$

where matrices $\boldsymbol{\Delta}_{k,\text{sub}} = K_{\text{m}}^{-1/2}\,\text{diag}[1, e^{j\frac{2\pi}{M}\bar{\iota}_k}, \ldots, e^{j\frac{2\pi}{M}\bar{\iota}_k(M_{\text{u}}-1)}] \in \mathbb{C}^{M_{\text{u}}\times M_{\text{u}}}$ and $\boldsymbol{\mathcal{J}}_{\text{sub}} \triangleq [\mathbf{I}_{L_{\text{eff}}+1}, \mathbf{O}_{(M_{\text{u}}-L_{\text{eff}}-1)\times(L_{\text{eff}}+1)}^T]^T$ are submatrices of $\boldsymbol{\Delta}_k$ and $\boldsymbol{\mathcal{J}}$, respectively, whereas $\widetilde{\mathbf{S}}_k(n) = \text{diag}[\widetilde{\mathbf{s}}_k(n)]$ has been previously introduced. Relying on (36), we define the SNR associated to the kth user as follows

$$\text{SNR}_k \triangleq \frac{\mathbb{E}\left[\left\|\alpha_k\sqrt{M}e^{j\frac{2\pi}{M}\epsilon_k(nP+L_{\text{eff}})}\,\widetilde{\mathbf{S}}_k(n)\,\mathbf{W}_{\text{dft}}\,\boldsymbol{\Delta}_{k,\text{sub}}^*\,\boldsymbol{\mathcal{J}}_{\text{sub}}\,\mathbf{G}_{k,\text{left,mmoe}}^*\,\boldsymbol{\gamma}\right\|^2\right]}{\mathbb{E}\left[\left\|\mathbf{W}_{\text{dft}}\,\mathbf{R}_k\,\mathbf{B}_{\text{mmoe}}\,\mathbf{D}(n)\,\boldsymbol{\gamma}\right\|^2\right]} \tag{37}$$

$$= \frac{\sigma_s^2\,M\,|\alpha_k|^2}{\sigma_w^2\,\kappa}\,\frac{\boldsymbol{\gamma}^H\,\mathbf{G}_{k,\text{left, mmoe}}^T\,\mathbf{G}_{k,\text{left, mmoe}}^*\,\boldsymbol{\gamma}}{\boldsymbol{\gamma}^H\,\mathbf{F}_{\text{mmoe}}^T\,\mathbf{F}_{\text{mmoe}}^*\,\boldsymbol{\gamma}}$$

$$= \frac{1}{\sigma_w^2\kappa}\,\frac{\boldsymbol{\gamma}^H\,\mathbf{R}_{\mathbf{Q}_k\mathbf{Q}_k}\,\boldsymbol{\gamma}}{\boldsymbol{\gamma}^H\,\mathbf{F}_{\text{mmoe}}^T\,\mathbf{F}_{\text{mmoe}}^*\,\boldsymbol{\gamma}} - 1 \tag{38}$$

where we have exploited the fact that the noise term in (37) is white, with variance $\kappa \triangleq \sum_{i=0}^{N-1} \left(\mathbf{B}_{\text{mmoe}}\mathbf{B}_{\text{mmoe}}^H\right)_{i,i}$, and $\mathbf{R}_{\mathbf{Q}_k\mathbf{Q}_k} \triangleq \mathbb{E}\left[\mathbf{Q}_k^H(n)\,\mathbf{Q}_k(n)\right] \in \mathbb{C}^{Q(L_{\text{eff}}+1)\times Q(L_{\text{eff}}+1)}$ is the correlation matrix of $\mathbf{Q}_k(n)$. Maximizing (38) with respect to $\boldsymbol{\gamma}$ boils down to solving

$$\boldsymbol{\gamma}_{k,\text{opt}} = \arg\max_{\boldsymbol{\gamma}} \left\{\boldsymbol{\gamma}^H\,\mathbf{R}_{\mathbf{Q}_k\mathbf{Q}_k}\,\boldsymbol{\gamma}\right\} \quad \text{subject to} \quad \boldsymbol{\gamma}^H\,\mathbf{F}_{\text{mmoe}}^T\,\mathbf{F}_{\text{mmoe}}^*\,\boldsymbol{\gamma} = 1 \tag{39}$$

whose solution depends on k and is given by the eigenvector associated to the largest generalized eigenvalue of the matrix pair $(\mathbf{R}_{\mathbf{Q}_k\mathbf{Q}_k}, \mathbf{F}_{\text{mmoe}}^T\,\mathbf{F}_{\text{mmoe}}^*)$. The vector $\boldsymbol{\gamma}_{k,\text{opt}}$ can be estimated from received data either in batch or adaptive mode [20].

3.4. Fourth stage: per-user detection

At this point, eq. (36) can be equivalently written as

$$\mathbf{q}_k(n) = e^{j\frac{2\pi}{M}\epsilon_k(nP+L_{\text{eff}})}\,\boldsymbol{\Lambda}_k\,\mathbf{W}_{\text{dft}}\,\mathbf{s}_k(n) + \mathbf{d}_k(n) \tag{40}$$

where $\boldsymbol{\Lambda}_k \triangleq \sqrt{M}\,\alpha_k\,\text{diag}\left(\mathbf{W}_{\text{dft}}\,\boldsymbol{\Delta}_{k,\text{sub}}^*\,\boldsymbol{\mathcal{J}}_{\text{sub}}\,\mathbf{G}_{k,\text{left, mmoe}}^*\,\boldsymbol{\gamma}_{k,\text{opt}}\right)$ and $\mathbf{d}_k(n) \triangleq \mathbf{W}_{\text{dft}}\,\mathbf{R}_k\,\mathbf{B}_{\text{mmoe}}\,\mathbf{D}(n)\,\boldsymbol{\gamma}_{k,\text{opt}}$. After refining the estimate of ϵ_k by using standard single-user frequency estimation techniques [33], estimating the equivalent shortened channel vector $\alpha_k\,\mathbf{G}_{k,\text{left, mmoe}}^*\,\boldsymbol{\gamma}_{k,\text{opt}}$, which also includes the I/Q imbalance parameter α_k, by means of conventional training-based channel estimators, under the assumption that $\boldsymbol{\Lambda}_k$ is nonsingular, the MMSE estimate $\widehat{\mathbf{s}}_k(n)$ of the symbol block $\mathbf{s}_k(n)$ transmitted by the kth user is given by

$$\widehat{\mathbf{s}}_k(n) = \sigma_s^2\,\alpha_k^*\,e^{-j\frac{2\pi}{M}\epsilon_k(nP+L_{\text{eff}})}\,\mathbf{W}_{\text{dft}}^H\,\boldsymbol{\Lambda}_k^*\,\mathbf{R}_{\mathbf{q}_k\mathbf{q}_k}^{-1}\,\mathbf{q}_k(n) \tag{41}$$

where $\mathbf{R}_{\mathbf{q}_k\mathbf{q}_k} \triangleq \mathbb{E}[\mathbf{q}_k(n)\,\mathbf{q}_k^H(n)]$ is the correlation matrix of $\mathbf{q}_k(n)$.

4. Simulation results

In this section, we present the results of Monte Carlo computer simulations, aimed at assessing the performance of the proposed multistage MMOE receiver, implemented in its data-dependent version. Since the second stage of such receiver (see Subsection 3.2) jointly performs multiuser CFO compensation and I/Q imbalance mitigation, in order to gain understanding about how these impairments separately affect the overall performances, we also considered two receivers adopting a simplified second-stage structure: the first one (referred to as "Only CFO compensation") performs only CFO

compensation, by employing in the second stage the data-independent matrix $\mathbf{B}_{\mathrm{mmoe}} = \mathbf{B}^{(f)}_{\mathrm{mmoe}} = \mathbf{\Psi}^{\dagger}$; the second one (referred to as "No CFO and I/Q compensation") does not take any countermeasure in the second stage against multiuser CFOs and I/Q imbalances.

In all the simulations, we considered a SC-IFDMA system employing a total of $M = 64$ QPSK-modulated subcarriers, with a CP of length $L_{\mathrm{cp}} = 4$, and a maximum of $K_{\mathrm{m}} = 4$ users. We assume that only $K = 3$ users are active, whose CFOs are set, unless otherwise specified, to $\epsilon_1 = 0$ and $\epsilon_2 = -\epsilon_3 = 0.25$. The BS is equipped with $N_{\mathrm{r}} = 8$ antennas and employs 2x oversampling ($N_{\mathrm{c}} = 2$). Each SC-IFDMA transmitter introduces severe I/Q imbalance, with $\Delta\phi = \pi/18$ and $\Delta a = 0.5$ [11], resulting in IRR = 5 dB. The user CIRs are of (maximum) order $L_{\max} = 8$, with the entries of $\mathbf{h}_k(\ell)$ modeled as independent and identically distributed (i.i.d.) circularly symmetric complex Gaussian random variables, having zero mean and variance $\sigma_h^2(\ell)$, with $\sigma_h^2(\ell) = \sigma_h^2(0)\,\exp(-0.1\,\ell)$, for $\ell \in \{0, 1, \ldots, L_{\max}\}$, where $\sigma_h^2(0)$ is chosen to ensure a unit average energy for $\mathbf{h}_k(\ell)$. The channels are kept fixed over each SC-IFDMA symbol, but are allowed to independently change from symbol to symbol. The additive noise vector $\mathbf{w}(m)$ is modeled as a zero-mean white complex circularly symmetric Gaussian vector. In all experiments, the first user is chosen as the desired one and the SNR is defined as $\mathrm{SNR} \triangleq \sigma_s^2/\sigma_w^2$.

The receivers under comparison differ only in the second stage, while performing channel shortening in the first stage (with the order of the channel shortening TEQ set to $L_{\mathrm{e}} = 7$), maximum SNR matched filtering in the third stage, and CFO compensation and I/Q imbalance mitigation (in the MMSE sense) only for the desired user in the fourth stage, assuming for data demodulation exact knowledge of $\alpha_k\,\mathbf{G}^{*}_{k,\mathrm{left,\ mmoe}}\,\boldsymbol{\gamma}_{k,\mathrm{opt}}$ (shortened channel). The matrices $\mathbf{R}_{\overline{\mathbf{rr}}}$ and $\mathbf{R}_{\mathbf{ZZ}}$, needed for the synthesis of the first and second stage, respectively, are estimated on the basis of a sample-size of $K_{\mathrm{s}} = 60$ SC-IFDMA symbols. Finally, since the system is not fully loaded ($K < K_{\mathrm{m}}$), with reference to the MMOE and "Only CFO compensation" receivers[5] we considered two different choices for L_{eff}: in the first case ("partial CP removal"), we set $L_{\mathrm{eff}} = 2 < L_{\mathrm{cp}}$ and, hence, $L_{\mathrm{unc}} = 2$, whereas in the second one ("total CP removal"), we set $L_{\mathrm{eff}} = L_{\mathrm{cp}}$ and, thus, $L_{\mathrm{unc}} = 0$.[6]

[5]The "No CFO and I/Q compensation" receiver works with $L_{\mathrm{eff}} = L_{\mathrm{cp}}$, since it can not take advantage of additional degrees of freedom in its second stage.

[6]In the case of total CP removal, the "Only CFO compensation" receiver exactly coincides with the one developed in [25].

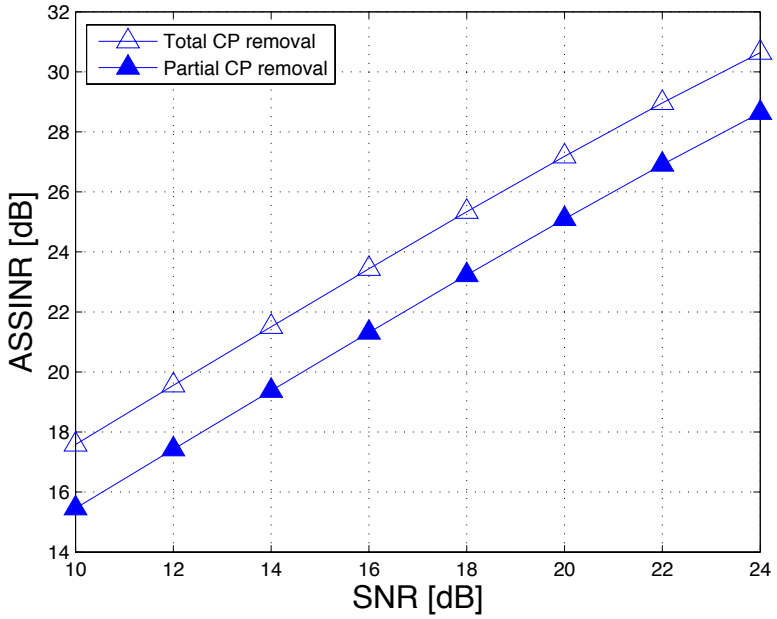

Figure 1: Average shortening SINR versus SNR.

The shortening performance of the receivers is measured by the average shortening SINR (ASSINR) at the shortening TEQ output, which is defined, on the basis of (8), as

$$\text{ASSINR} \triangleq \frac{\mathbb{E}\left[\left|\mathbf{g}_{1,\text{win}}^{H}\left[\alpha_1\,\overline{\mathbf{u}}_{1,\text{win}}(m)+\beta_1\,\overline{\mathbf{u}}_{1,\text{win}}^{*}(m)\right]\right|^2\right]}{\mathbb{E}\left[\left|\mathbf{g}_{1,\text{wall}}^{H}\left[\alpha_1\,\overline{\mathbf{u}}_{1,\text{wall}}(m)+\beta_1\,\overline{\mathbf{u}}_{1,\text{wall}}^{*}(m)\right]+v(m)\right|^2\right]}. \quad (42)$$

Note that the ASSINR definition (42) does not distinguish between the desired signal and I/Q imbalance. Moreover, as an overall performance figure, we employed the average (over all subcarriers) BER (ABER). Both ASSINR and ABER values are obtained by averaging the results over 3000 SC-IFDMA symbols and 1000 Monte Carlo trials.

In the first experiment, we assessed the ASSINR and ABER performances of the receivers as a function of the SNR. In particular, Fig. 1 reports the ASSINR values versus SNR, in the case of total and partial CP removal: we do not distinguish among the different receivers, since their shortening performances, depending only on the first stage, turn out to be coincident. It can be seen that the shortening stage performs satisfactorily, notwithstanding the presence of the CFOs and I/Q imbalances, assuring val-

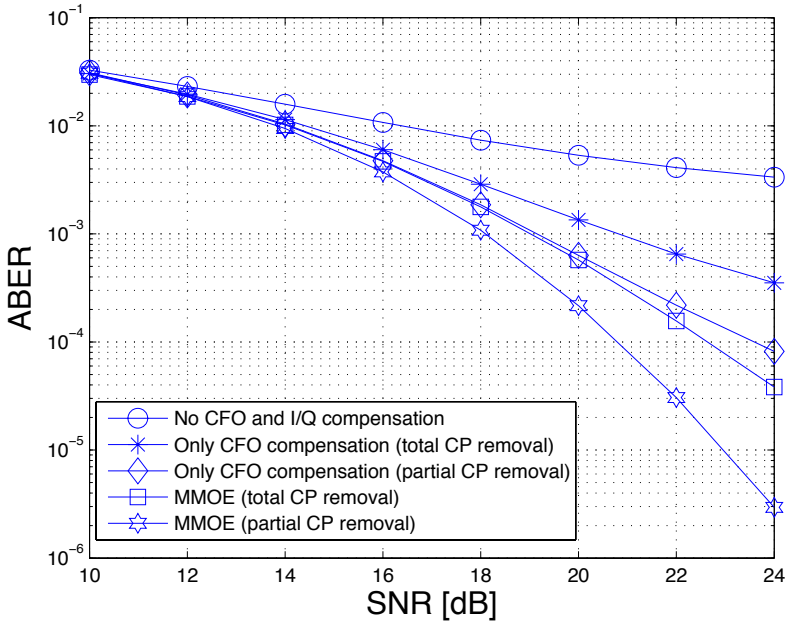

Figure 2: Average BER versus SNR.

ues of ASSINR which, for the considered range of SNR values, scale almost linearly with the SNR; it is worthwhile to note that further increases of the SNR would reveal, as expected, a saturation effect in the ASSINR, due to the finite sample-size $K_{\rm s}$ adopted for $\mathbf{R}_{\overline{\mathbf{rr}}}$ estimation, which can be reduced (if needed) by simply increasing $K_{\rm s}$.

It is interesting to observe that, compared to total CP removal, partial CP removal pays an ASSINR penalty of about 3 dB, independently of the SNR, since the choice $L_{\rm eff} < L_{\rm cp}$ introduces noise enhancement [20] during the channel shortening process. However, it must be remembered that partial CP removal increases the degrees of freedom at our disposal to counteract CFO and I/Q imbalance effects in the second stage. A more meaningful comparison must be necessarily carried out in terms of ABER at the output of the overall receiver, which is reported in Fig. 2, as a function of SNR. Results clearly show, as expected, that the "No CFO and I/Q compensation" receiver exhibits poor overall performances; on the contrary, the MMOE receiver with partial CP removal exhibits the best overall performances. It is interesting to observe that even the simplified "Only CFO compensation" receiver, especially when implemented with partial CP removal, is able to provide a significant performance gain over the "No CFO and I/Q compensation" one, since it allows to recover the loss of user orthogonality due to

CFOs. Its performance degradation with respect to the MMOE one for increasing SNR values is essentially due to the fact that no countermeasure is taken in the "Only CFO compensation" receiver to mitigate multiuser I/Q imbalance, which is the predominant source of performance degradation for vanishingly small noise. Finally, by comparing results of Figs. 1 and 2, it is confirmed that partial CP removal, although inferior in terms of channel shortening capabilities due to noise enhancements, provides better overall ABER performances, since it allows one to gain important degrees of freedom to reliably mitigate I/Q imbalances.

To check the robustness of the proposed receiver against possible CFO estimation errors, in the second experiment we report the ABER performance of the MMOE and "Only CFO compensation" receivers when the true CFO values are affected by a random perturbation; specifically, we replace ϵ_k in the construction of $\mathbf{\Psi}$ in (32) and (33) with $\widehat{\epsilon}_k = \epsilon_k + \Delta\epsilon_k$, for $k \in \{1, 2, \ldots, K\}$, where $\Delta\epsilon_1, \Delta\epsilon_2, \ldots, \Delta\epsilon_K$ are i.i.d. uniform random variables in $(-\Delta\epsilon_{\max}, \Delta\epsilon_{\max})$. The results are reported in Fig. 3 for the MMOE and "Only CFO compensation" receivers, since the "No CFO and I/Q compensation" receiver exhibits a fixed ABER, roughly equal to $5 \cdot 10^{-3}$, since it does not perform any CFO compensation. It is interesting to observe that CFO perturbations not exceeding $\Delta\epsilon_{\max} = 0.03$ (which is a reasonable value for CFO estimation algorithms) have only a slight impact on the performance of the receivers under comparison, while higher CFO perturbation values determine a more significant performance degradation, due to imperfect CFO compensation.

Finally, in the third experiment we assessed the sensitivity of the ABER performances to different values of the user CFOs. In particular, we considered a slightly modified scenario, where the CFO of the desired user is kept fixed at $\epsilon_1 = 0$, whereas those of the MAI users are chosen as $\epsilon_2 = -\epsilon_2 = \epsilon$, with ϵ chosen in the range $0 \div 0.45$ with step 0.05. Results of Fig. 4 (for SNR = 20 dB) show that all the receivers exhibit some performance degradation as ϵ increases; however, observe that the MMOE receiver, especially when the CP is partially removed, is remarkably robust against CFOs variations, assuring satisfactory performances in the whole range of ϵ values. It is interesting to observe that, for values of ϵ approaching zero, all the receivers performing total/partial CP removal perform similarly: indeed, when $\epsilon \to 0$, it can be proven mathematically [see (20)] that not only the MAI users, but also their I/Q contributions become orthogonal to the desired one, making the compensation/mitigation carried out in the second stage essentially irrelevant.

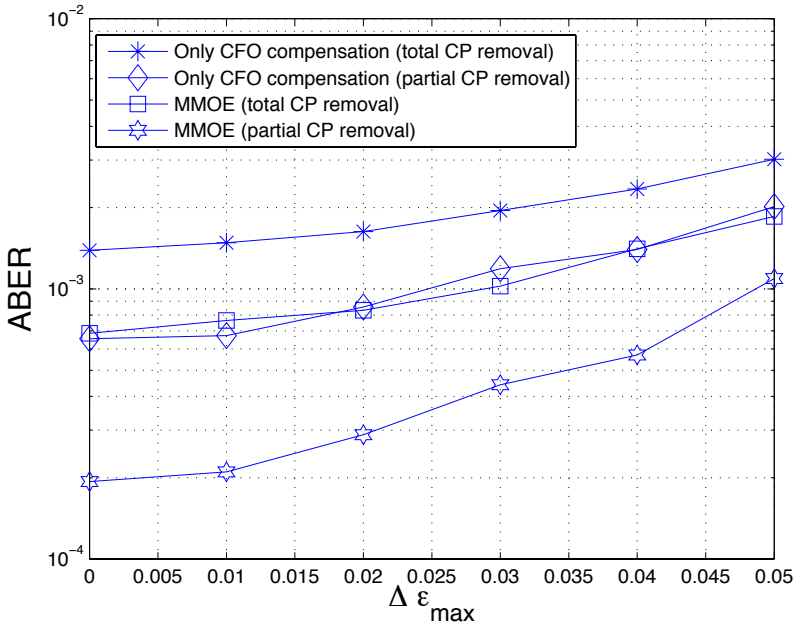

Figure 3: Average BER versus $\Delta\epsilon_{\max}$.

5. Conclusions

In this paper, we proposed a blind receiver for the uplink of a SC-IFDMA system, which jointly accounts for the combined effects of timing errors and channel dispersion, I/Q imbalance introduced at each transmitter, and CFOs between the transmitted and received signals. The proposed receiver is arranged in a multistage configuration, which orderly performs: (i) blind multiuser MMOE channel shortening in the time domain, without requiring any *a priori* knowledge about the channels to be shortened; (ii) joint multiuser MMOE compensation of CFOs and mitigation of I/Q impairments; (iii) per-user blind maximum SNR-based matched filtering; (iv) MMSE symbol detection for the desired user. Numerical results show that the proposed receiver exhibits a remarkable robustness against actual CFO values as well as CFO perturbations due to estimation errors.

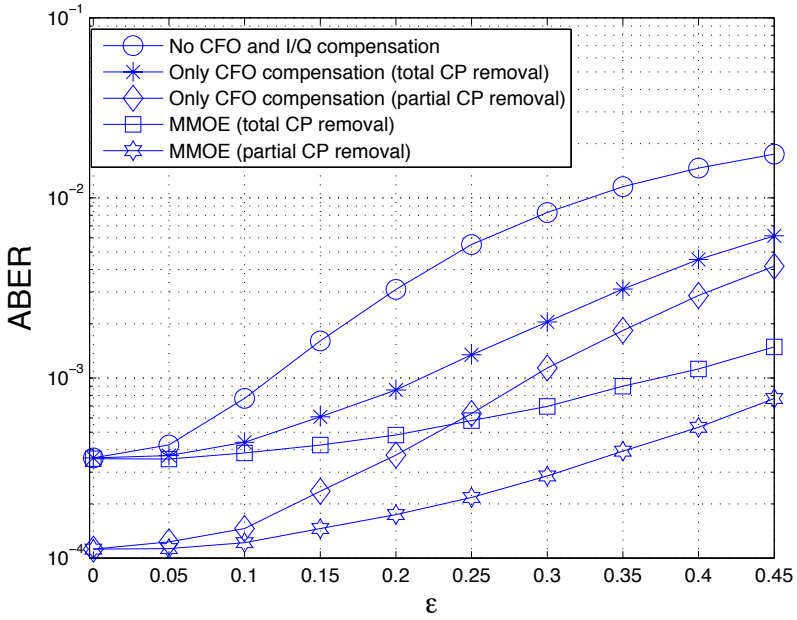

Figure 4: Average BER versus ϵ.

Appendix A. Expression of the matrix $\mathbf{Z}(n)$

Using (8), one obtains

$$\mathbf{Z}(n) = \sum_{k=1}^{K} e^{j\frac{2\pi}{M}\epsilon_k(nP+L_{\text{eff}})}\, \mathbf{\Omega}_k \left[\alpha_k\, \overline{\mathbf{U}}_{k,\text{left}} + \beta_k\, \overline{\mathbf{U}}^*_{k,\text{left}}\right] \mathbf{G}^*_{k,\text{left,mmoe}} + \mathbf{D}(n) \tag{A.1}$$

where $\mathbf{\Omega}_k$ is given by (23), $\overline{\mathbf{U}}_{k,\text{left}}(n) \triangleq [\overline{\mathbf{u}}_{k,\text{left}}(nP+L_{\text{eff}}), \ldots, \overline{\mathbf{u}}_{k,\text{left}}(nP+P-1)]^T \in \mathbb{C}^{N\times(L_{\text{eff}}+1)}$, and $\mathbf{D}(n) \triangleq [\mathbf{d}(nP+L_{\text{eff}}), \ldots, \mathbf{d}(nP+P-1)]^T \in \mathbb{C}^{N\times Q(L_{\text{eff}}+1)}$. Observing that $\overline{\mathbf{u}}_{k,\text{left}}(m) = [u_k(m),\, u_k(m-1), \ldots, u_k(m-L_{\text{eff}})]^T \in \mathbb{C}^{L_{\text{eff}}+1}$ and the CP is a replica of the last $L_{\text{cp}} \geq L_{\text{eff}}$ samples of the SC-IFDMA symbol (1), it can be verified that

$$\overline{\mathbf{U}}_{k,\text{left}}(n) = \mathbf{T}_{\text{unc}}\, \mathbf{U}_{k,\text{left}}(n) \tag{A.2}$$

where $\mathbf{T}_{\text{unc}} \triangleq [\mathbf{I}^T_{\text{unc}}, \mathbf{I}_M]^T \in \mathbb{R}^{N\times M}$, with $\mathbf{I}_{\text{unc}} \in \mathbb{R}^{L_{\text{unc}}\times M}$ collecting the last L_{unc} rows of $\mathbf{I}_M$ and $L_{\text{unc}} \triangleq L_{\text{cp}} - L_{\text{eff}}$, whereas $\mathbf{U}_{k,\text{left}}(n) \in \mathbb{C}^{M\times(L_{\text{eff}}+1)}$ the

$M \times (L_{\rm eff}+1)$ complex matrix

$$\mathbf{U}_{k,\rm left}(n) = \begin{bmatrix} u_k(nP+L_{\rm cp}) & u_k(nP+P-1) & \dots & u_k(nP+L_{\rm cp}-L_{\rm eff}) \\ u_k(nP+L_{\rm cp}+1) & u_k(nP+L_{\rm cp}) & \dots & u_k(nP+L_{\rm cp}-L_{\rm eff}+1) \\ \vdots & \ddots & \dots & \vdots \\ u_k(nP+P-1) & u_k(nP+P-2) & \dots & u_k(nP+P-L_{\rm eff}-1) \end{bmatrix} \tag{A.3}$$

is a column-wise circulant matrix. We observe that (A.3) can be re-expressed as $\mathbf{U}_{k,\rm left}(n) = \boldsymbol{\mathcal{U}}_{k,\rm left}(n)\,\boldsymbol{\mathcal{J}}$, where $\boldsymbol{\mathcal{U}}_{k,\rm left}(n) \in \mathbb{C}^{M\times M}$ is the circulant matrix having $[u_k(nP+L_{\rm cp}), u_k(nP+L_{\rm cp}+1), \dots, u_k(nP+P-1)]^T = \mathbf{W}_k\,\widetilde{\mathbf{s}}_k(n)$ as first column [see (1)] and $\boldsymbol{\mathcal{J}} \triangleq [\mathbf{I}_{L_{\rm eff}+1}, \mathbf{O}_{(L_{\rm eff}+1)\times(M-L_{\rm eff}-1)}]^T \in \mathbb{R}^{M\times(L_{\rm eff}+1)}$. Therefore, by using the fact that the circulant matrix $\boldsymbol{\mathcal{U}}_{k,\rm left}(n)$ is diagonalized by the M-point DFT, it can be shown from (A.1) and (A.2) that

$$\begin{aligned}\mathbf{Z}(n) = \sqrt{M}\sum_{k=1}^{K} e^{j\frac{2\pi}{M}\epsilon_k(nP+L_{\rm eff})}\,\boldsymbol{\Omega}_k\,\mathbf{T}_{\rm unc}\Big\{&\alpha_k\ \mathbf{W}_k\,\widetilde{\mathbf{S}}_k(n)\,\mathbf{W}_k^H \\ &+\beta_k\ \Big[\mathbf{W}_k\,\widetilde{\mathbf{S}}_k(n)\,\mathbf{W}_k^H\Big]^*\Big\}\,\boldsymbol{\mathcal{J}}\,\mathbf{G}^*_{k,\rm left,mmoe} + \mathbf{D}(n)\end{aligned} \tag{A.4}$$

where $\widetilde{\mathbf{S}}_k(n) \triangleq \mathrm{diag}[\widetilde{\mathbf{s}}_k(n)] \in \mathbb{C}^{M_{\rm u}\times M_{\rm u}}$. Moreover, it is verified that $\mathbf{W}_k = \boldsymbol{\Delta}_k\left(\mathbf{1}_{K_{\rm m}} \otimes \mathbf{W}_{\rm dft}^{-1}\right)$, where $\boldsymbol{\Delta}_k$ is give by (24). Thus, let $\boldsymbol{\mathcal{S}}_k(n) \in \mathbb{C}^{M_{\rm u}\times M_{\rm u}}$ be the circulant matrix having the time-domain information block $\mathbf{s}_k(n)$ as first column, and remembering that $\widetilde{\mathbf{s}}_k(n) = \mathbf{W}_{\rm dft}\,\mathbf{s}_k(n)$, one obtains

$$\mathbf{W}_k\,\widetilde{\mathbf{S}}_k(n)\,\mathbf{W}_k^H = \frac{1}{\sqrt{M_{\rm u}}}\,\boldsymbol{\Delta}_k\,\left[\mathbf{1}_{K_{\rm m}} \otimes \mathbf{1}_{K_{\rm m}}^T \otimes \boldsymbol{\mathcal{S}}_k(n)\right]\,\boldsymbol{\Delta}_k^*\,. \tag{A.5}$$

Substituting (A.5) into (A.4), it turns out that

$$\begin{aligned}\mathbf{Z}(n) = \sqrt{\frac{M}{M_{\rm u}}}\sum_{k=1}^{K} e^{j\frac{2\pi}{M}\epsilon_k(nP+L_{\rm eff})}\,\Big\{&\alpha_k\,\boldsymbol{\Psi}_k\left[\mathbf{1}_{K_{\rm m}} \otimes \mathbf{1}_{K_{\rm m}}^T \otimes \boldsymbol{\mathcal{S}}_k(n)\right]\boldsymbol{\Delta}_k^* \\ &+\beta_k\,\boldsymbol{\Psi}_{k,\rm mir}\left[\mathbf{1}_{K_{\rm m}} \otimes \mathbf{1}_{K_{\rm m}}^T \otimes \boldsymbol{\mathcal{S}}_k^*(n)\right]\boldsymbol{\Delta}_k\Big\}\,\boldsymbol{\mathcal{J}}\,\mathbf{G}^*_{k,\rm left,mmoe} + \mathbf{D}(n)\end{aligned} \tag{A.6}$$

with $\boldsymbol{\Psi}_k \triangleq \boldsymbol{\Omega}_k\,\mathbf{T}_{\rm unc}\,\boldsymbol{\Delta}_k \in \mathbb{C}^{N\times M}$ and $\boldsymbol{\Psi}_{k,\rm mir} \triangleq \boldsymbol{\Omega}_k\,\mathbf{T}_{\rm unc}\,\boldsymbol{\Delta}_k^* \in \mathbb{C}^{N\times M}$. By partitioning $\boldsymbol{\Psi}_k = [\boldsymbol{\Psi}_k^{(1)}, \boldsymbol{\Psi}_k^{(2)}, \dots, \boldsymbol{\Psi}_k^{(K_{\rm m})}]$, with $\boldsymbol{\Psi}_k^{(\ell)} \in \mathbb{C}^{N\times M_{\rm u}}$, and $\boldsymbol{\Psi}_{k,\rm mir} = [\boldsymbol{\Psi}_{k,\rm mir}^{(1)}, \boldsymbol{\Psi}_{k,\rm mir}^{(2)}, \dots, \boldsymbol{\Psi}_{k,\rm mir}^{(K_{\rm m})}]$, with $\boldsymbol{\Psi}_{k,\rm mir}^{(\ell)} \in \mathbb{C}^{N\times M_{\rm u}}$, eq. (A.6) can be equivalently rewritten as (20).

Appendix B. Second-order statistical characterization of $\mathbf{Z}(n)$

Under our assumptions, it is easily seen that $\mathbf{Z}(n)$ is a zero-mean complex random matrix, whose second-order moments are defined in terms of two matrices: the correlation matrix $\mathbf{R}_{\mathbf{ZZ}} \triangleq \mathbb{E}[\mathbf{Z}(n)\,\mathbf{Z}^H(n)] \in \mathbb{C}^{N\times N}$ and the conjugate correlation matrix $\mathbf{R}_{\mathbf{ZZ}^*}(n) \triangleq \mathbb{E}[\mathbf{Z}(n)\,\mathbf{Z}^T(n)] \in \mathbb{C}^{N\times N}$. Accounting for (20), one has

$$\begin{aligned}\mathbf{R}_{\mathbf{ZZ}} &= \mathbf{\Psi}\,\mathbb{E}[\mathbf{A}(n)\,\mathbf{A}^H(n)]\,\mathbf{\Psi}^H + \mathbf{\Psi}\,\mathbb{E}[\mathbf{A}(n)\,\mathbf{A}^H_{\mathrm{mir}}(n)]\,\mathbf{\Psi}^H_{\mathrm{mir}} \\ &\quad + \mathbf{\Psi}_{\mathrm{mir}}\,\mathbb{E}[\mathbf{A}_{\mathrm{mir}}(n)\,\mathbf{A}^H(n)]\,\mathbf{\Psi}^H + \mathbf{\Psi}_{\mathrm{mir}}\,\mathbb{E}[\mathbf{A}_{\mathrm{mir}}(n)\,\mathbf{A}^H_{\mathrm{mir}}(n)]\,\mathbf{\Psi}^H_{\mathrm{mir}} + \mathbf{R}_{\mathbf{DD}}\end{aligned} \tag{B.1}$$

where $\mathbf{R}_{\mathbf{DD}} \triangleq \mathbb{E}[\mathbf{D}(n)\,\mathbf{D}^H(n)] \in \mathbb{C}^{N\times N}$. It follows from (25) that the matrix $\mathbb{E}[\mathbf{A}(n)\,\mathbf{A}^H(n)] \in \mathbb{C}^{KM_{\mathrm{u}}\times KM_{\mathrm{u}}}$ is block diagonal, whose kth main diagonal block is given by $\mathbb{E}[\mathbf{A}_k(n)\,\mathbf{A}^H_k(n)] \in \mathbb{C}^{M_{\mathrm{u}}\times M_{\mathrm{u}}}$, for $k \in \{1,2,\ldots,K\}$. By virtue of (27), one obtains

$$\begin{aligned}\mathbb{E}[\mathbf{A}_k(n)\,\mathbf{A}^H_k(n)] &= \frac{M}{M_{\mathrm{u}}}\,|\alpha_k|^2\,\boldsymbol{\mathcal{C}}_k\left(\mathbf{I}_{Q(L_{\mathrm{eff}}+1)} \otimes \mathbb{E}[\mathbf{s}_k(n)\,\mathbf{s}^H_k(n)]\right)\boldsymbol{\mathcal{C}}^H_k \\ &= \sigma_s^2\,\frac{M}{M_{\mathrm{u}}}\,|\alpha_k|^2\,\boldsymbol{\mathcal{C}}_k\,\boldsymbol{\mathcal{C}}^H_k\end{aligned} \tag{B.2}$$

where $\mathbf{C}_k \triangleq [\{\mathbf{C}^{(1)}_k\}^T, \{\mathbf{C}^{(2)}_k\}^T, \ldots, \{\mathbf{C}^{(K_{\mathrm{m}})}_k\}^T]^T = \mathbf{\Delta}^*_k\,\boldsymbol{\mathcal{J}}\,\mathbf{G}^*_{k,\mathrm{left,mmoe}}$, with $\mathbf{C}^{(\ell)}_k \in \mathbb{C}^{M_{\mathrm{u}}\times Q(L_{\mathrm{eff}}+1)}$, $\sum_{\ell=1}^{K_{\mathrm{m}}} \mathbf{C}^{(\ell)}_k \triangleq [\mathbf{c}^{(1)}_k, \mathbf{c}^{(2)}_k, \ldots, \mathbf{c}^{(Q(L_{\mathrm{eff}}+1))}_k]$, we have used the fact that $\boldsymbol{\mathcal{S}}_k(n)$ is a circulant matrix having $\mathbf{s}_k(n)$ as first column and, thus, $\boldsymbol{\mathcal{S}}_k(n)\,\mathbf{c}^{(q)}_k = \boldsymbol{\mathcal{C}}^{(q)}_k\,\mathbf{s}_k(n)$, where $\boldsymbol{\mathcal{C}}^{(q)}_k \in \mathbb{C}^{M_{\mathrm{u}}\times M_{\mathrm{u}}}$ is the circulant matrix having $\mathbf{c}^{(q)}_k$ as first column, for $q \in \{1,2,\ldots,Q(L_{\mathrm{eff}}+1)\}$, and, finally, $\boldsymbol{\mathcal{C}}_k \triangleq [\boldsymbol{\mathcal{C}}^{(1)}_k, \boldsymbol{\mathcal{C}}^{(2)}_k, \ldots, \boldsymbol{\mathcal{C}}^{(Q(L_{\mathrm{eff}}+1))}_k] \in \mathbb{C}^{M_{\mathrm{u}}\times M_{\mathrm{u}}Q(L_{\mathrm{eff}}+1)}$. Similarly, it comes from (28) and (26) that the matrix $\mathbb{E}[\mathbf{A}_{\mathrm{mir}}(n)\,\mathbf{A}^H_{\mathrm{mir}}(n)] \in \mathbb{C}^{KM_{\mathrm{u}}\times KM_{\mathrm{u}}}$ is block diagonal, whose kth main diagonal block is given by

$$\begin{aligned}\mathbb{E}[\mathbf{A}_{k,\mathrm{mir}}(n)\,\mathbf{A}^H_{k,\mathrm{mir}}(n)] &= \frac{M}{M_{\mathrm{u}}}\,|\beta_k|^2\,\boldsymbol{\mathcal{C}}_{k,\mathrm{mir}}\left(\mathbf{I}_{Q(L_{\mathrm{eff}}+1)} \otimes \mathbb{E}^*[\mathbf{s}_k(n)\,\mathbf{s}^H_k(n)]\right)\boldsymbol{\mathcal{C}}^H_{k,\mathrm{mir}} \\ &= \sigma_s^2\,\frac{M}{M_{\mathrm{u}}}\,|\beta_k|^2\,\boldsymbol{\mathcal{C}}_{k,\mathrm{mir}}\,\boldsymbol{\mathcal{C}}^H_{k,\mathrm{mir}}\end{aligned} \tag{B.3}$$

where $\mathbf{C}_{k,\mathrm{mir}} \triangleq [\{\mathbf{C}^{(1)}_{k,\mathrm{mir}}\}^T, \{\mathbf{C}^{(2)}_{k,\mathrm{mir}}\}^T, \ldots, \{\mathbf{C}^{(K_{\mathrm{m}})}_{k,\mathrm{mir}}\}^T]^T = \mathbf{\Delta}_k\,\boldsymbol{\mathcal{J}}\,\mathbf{G}^*_{k,\mathrm{left,mmoe}}$, with $\mathbf{C}^{(\ell)}_{k,\mathrm{mir}} \in \mathbb{C}^{M_{\mathrm{u}}\times Q(L_{\mathrm{eff}}+1)}$, $\sum_{\ell=1}^{K_{\mathrm{m}}} \mathbf{C}^{(\ell)}_{k,\mathrm{mir}} \triangleq [\mathbf{c}^{(1)}_{k,\mathrm{mir}}, \mathbf{c}^{(2)}_{k,\mathrm{mir}}, \ldots, \mathbf{c}^{(Q(L_{\mathrm{eff}}+1))}_{k,\mathrm{mir}}]$, $\boldsymbol{\mathcal{C}}^{(q)}_{k,\mathrm{mir}} \in \mathbb{C}^{M_{\mathrm{u}}\times M_{\mathrm{u}}}$ is the circulant matrix having $\mathbf{c}^{(q)}_{k,\mathrm{mir}}$ as first column, and,

finally, $\boldsymbol{\mathcal{C}}_{k,\mathrm{mir}} \triangleq [\boldsymbol{\mathcal{C}}_{k,\mathrm{mir}}^{(1)}, \boldsymbol{\mathcal{C}}_{k,\mathrm{mir}}^{(2)}, \ldots, \boldsymbol{\mathcal{C}}_{k,\mathrm{mir}}^{(Q(L_{\mathrm{eff}}+1))}] \in \mathbb{C}^{M_{\mathrm{u}} \times M_{\mathrm{u}} Q(L_{\mathrm{eff}}+1)}$. In the same way, from (27), (28), (25), and (26), one has $\mathbb{E}[\mathbf{A}_{\mathrm{mir}}(n)\,\mathbf{A}^H(n)] = \mathbb{E}[\mathbf{A}(n)\,\mathbf{A}_{\mathrm{mir}}^H(n)] = \mathbf{O}_{KM_{\mathrm{u}} \times KM_{\mathrm{u}}}$, since $\mathbb{E}[\mathbf{A}(n)\,\mathbf{A}_{\mathrm{mir}}^H(n)]$ is block diagonal, whose kth main diagonal block is given by

$$\begin{aligned}\mathbb{E}[\mathbf{A}_k(n)\,\mathbf{A}_{k,\mathrm{mir}}^H(n)] &= \frac{M}{M_{\mathrm{u}}}\,\alpha_k\,\beta_k^*\,\boldsymbol{\mathcal{C}}_k\left(\mathbf{I}_{Q(L_{\mathrm{eff}}+1)} \otimes \mathbb{E}[\mathbf{s}_k(n)\,\mathbf{s}_k^T(n)]\right)\boldsymbol{\mathcal{C}}_{k,\mathrm{mir}}^H \\ &= \mathbf{O}_{M_{\mathrm{u}} \times M_{\mathrm{u}}}\,. \end{aligned} \tag{B.4}$$

With a similar reasoning, one has

$$\begin{aligned}\mathbf{R}_{\mathbf{Z}\mathbf{Z}^*}(n) &= \boldsymbol{\Psi}\,\mathbb{E}[\mathbf{A}(n)\,\mathbf{A}^T(n)]\,\boldsymbol{\Psi}^T + \boldsymbol{\Psi}\,\mathbb{E}[\mathbf{A}(n)\,\mathbf{A}_{\mathrm{mir}}^T(n)]\,\boldsymbol{\Psi}_{\mathrm{mir}}^T \\ &\quad + \boldsymbol{\Psi}_{\mathrm{mir}}\,\mathbb{E}[\mathbf{A}_{\mathrm{mir}}(n)\,\mathbf{A}^T(n)]\,\boldsymbol{\Psi}^T + \boldsymbol{\Psi}_{\mathrm{mir}}\,\mathbb{E}[\mathbf{A}_{\mathrm{mir}}(n)\,\mathbf{A}_{\mathrm{mir}}^T(n)]\,\boldsymbol{\Psi}_{\mathrm{mir}}^T \end{aligned} \tag{B.5}$$

where $\mathbb{E}[\mathbf{A}(n)\,\mathbf{A}^T(n)] = \mathbb{E}[\mathbf{A}_{\mathrm{mir}}(n)\,\mathbf{A}_{\mathrm{mir}}^T(n)] = \mathbf{O}_{KM_{\mathrm{u}} \times KM_{\mathrm{u}}}$, whereas the matrix $\mathbb{E}[\mathbf{A}_{\mathrm{mir}}(n)\,\mathbf{A}^T(n)] = \mathbb{E}[\mathbf{A}(n)\,\mathbf{A}_{\mathrm{mir}}^T(n)]$ is block diagonal, whose kth main diagonal block is given by

$$\mathbb{E}[\mathbf{A}_k(n)\,\mathbf{A}_{k,\mathrm{mir}}^T(n)] = \sigma_s^2\,\frac{M}{M_{\mathrm{u}}}\,\alpha_k\,\beta_k\,e^{j\frac{4\pi}{M}\epsilon_k(nP+L_{\mathrm{eff}})}\,\boldsymbol{\mathcal{C}}_k\,\boldsymbol{\mathcal{C}}_{k,\mathrm{mir}}^T \tag{B.6}$$

which shows that the conjugate correlation matrix of $\mathbf{Z}(n)$ is nonzero, i.e., the random matrix $\mathbf{Z}(n)$ is improper [26] and TV.

References

[1] T. Frank, A. Klein, and E. Costa, "IFDMA: a scheme combining the advantages of OFDMA and CDMA," *IEEE Wireless Commun.*, pp. 9–17, June 2007.

[2] M. Morelli, C.-C.J. Kuo, and M.-O. Pun, "Synchronization techniques for orthogonal frequency division multiple access (OFDMA): a tutorial review," *Proc. IEEE*, vol. 95, pp. 1394–1427, July 2007.

[3] Y. Zhu and K.B. Letaief, "CFO estimation and compensation in SC-IFDMA systems," *IEEE Trans. Wireless Commun.*, vol. 9, pp. 3200–3212, Oct. 2010.

[4] Y. Yoshida, K. Hayashi, H. Sakai, and W. Bocquet, "Analysis and compensation of transmitter IQ imbalances in OFDMA and SC-FDMA systems", *IEEE Trans. Signal Process.*, vol. 57, pp. 3119–3129, Aug. 2009.

[5] L. Angrisani, I. Ghidini, and M. Vadursi, "A New Method for I/Q Impairment Evaluation in OFDM Transmitters", *IEEE Trans. on Instrumentation and Measurement*, vol. 55, pp. 1480–1486, Oct. 2006.

[6] L. Angrisani, M. D'Arco, and M. Vadursi, "Clustering-based Method for Detecting and Evaluating I/Q Impairments in Radio Frequency Digital Transmitters", *IEEE Trans. on Instrumentation and Measurement*, vol. 56, pp. 2139–2146, Dec. 2007.

[7] L. Angrisani, M. D'Arco, and M. Vadursi, "Error Vector-Based Measurement Procedures for RF Digital Transmitters Troubleshooting", *IEEE Trans. on Instrumentation and Measurement*, vol. 54, pp. 1381–1387, Aug. 2005.

[8] P.J.W. Melsa, R.C. Younce, and C.E. Rohrs, "Impulse response shortening for discrete multitone transceivers," *IEEE Trans. Commun.*, vol. 44, pp. 1662–1672, Dec. 1996.

[9] G. Xing, M. Shen, and H. Liu, "Frequency offset and I/Q imbalance compensation for direct-conversion receivers," *IEEE Trans. Wireless Commun.*, vol. 4, pp. 673–680, Mar. 2005.

[10] D. Tandur and M. Moonen, "Joint adaptive compensation of transmitter and receiver IQ imbalance under carrier frequency offset in OFDM-based systems", *IEEE Trans. Signal Process.*, vol. 55, pp. 5246–5252, Nov. 2007.

[11] I. Barhumi and M. Moonen, "IQ-imbalance compensation for OFDM in the presence of IBI and carrier-frequency offset", *IEEE Trans. Signal Process.*, vol. 55, pp. 256–266, Jan. 2007.

[12] D. Daly, C. Heneghan, and A.D. Fagan, "Minimum mean-squared error impulse response shortening for discrete multitone transceivers", *IEEE Trans. Signal Process.*, vol. 52, pp. 301-306, Jan. 2004.

[13] G. Arslan, B. Evans, and S. Kiaei, "Equalization for discrete multitone transceivers to maximize bit rate", *IEEE Trans. Signal Process.*, vol. 49, pp. 3123-3135, Dec. 2001.

[14] S. Celebi, "Interblock interference (IBI) minimizing time-domain equalizer (TEQ) for OFDM", *IEEE Signal Process. Lett.*, vol. 10, pp. 232–234, Aug. 2003.

[15] R.K. Martin, J. Balakrishnan, W.A. Sethares, and C.R. Johnson, "A blind adaptive TEQ for multicarrier systems", *IEEE Signal Process. Lett.*, vol. 9, pp. 341–343, Nov. 2002.

[16] J. Balakrishnan, R.K. Martin, and C.R. Johnson, "Blind adaptive channel shortening by sum-squared auto-correlation minimization (SAM)", *IEEE Trans. Signal Process.*, vol. 51, pp. 3086–3093, Dec. 2003.

[17] T. Miyajima and Z. Ding, "Second-order statistical approaches to channel shortening in multicarrier systems", *IEEE Trans. Signal Process.*, vol. 52, pp. 3253–3264, Nov. 2004.

[18] R.K. Martin, J.M. Walsh, and C.R. Johnson, "Low-complexity MIMO

blind adaptive channel shortening", *IEEE Trans. Signal Process.*, vol. 53, pp. 1324-1334, Apr. 2005.

[19] R.K. Martin, "Joint blind adaptive carrier frequency offset estimation and channel shortening", *IEEE Trans. Signal Process.*, vol. 54, pp. 4194-4203, Nov. 2006.

[20] D. Darsena and F. Verde, "Minimum-mean-output-energy blind adaptive channel shortening for multicarrier SIMO transceivers," *IEEE Trans. Signal Process.*, vol. 55, pp. 5755–5771, Jan. 2007.

[21] R.K. Martin, G. Ysebaert, and K. Vanbleu, "Bit error rate minimizing channel shortening equalizers for cyclic prefixed systems", *IEEE Trans. Signal Process.*, vol. 55, pp. 2605-2616, June 2007.

[22] D. Darsena, G. Gelli, L. Paura, and F. Verde, "Blind periodically time-varying MMOE channel shortening for OFDM systems," in *Proc. IEEE International Conf. Acoustics, Speech and Signal Proc.*, Prague, Czech Republic, May 2011, pp. 3576– 3579.

[23] D. Darsena, G. Gelli, L. Paura, and F. Verde, "Blind channel shortening for space-time-frequency block coded MIMO-OFDM systems," *IEEE Trans. Wireless Commun.*, vol. 11, pp. 1022 – 1033, Mar. 2012.

[24] T. Miyajima and Z. Ding, "Subcarrier nulling algorithms for channel shortening in uplink OFDMA systems", *IEEE Trans. Signal Process.*, vol. 60, pp. 2374–2385, May 2012.

[25] D. Darsena, G. Gelli, L. Paura, and F. Verde, "Blind channel shortening for uplink SC-IFDMA operating over highly-dispersive channels," in *Proc. IEEE International Conf. Commun.*, Budapest, Hungary, June 2013, pp. 3174–3178.

[26] F.D. Neeser and J.L. Massey, "Proper complex random processes with applications to information theory," *IEEE Trans. Information Theory*, pp. 1293–1302, July 1993.

[27] B. Picinbono and P. Chevalier, "Widely linear estimation with complex data," *IEEE Trans. Signal Process.*, vol. 43, pp. 2030–2033, Aug. 1995.

[28] A.S. Cacciapuoti, G. Gelli, L. Paura, F. Verde, "Finite-sample performance analysis of widely-linear multiuser receivers for DS-CDMA systems", *IEEE Trans. Signal Process.*, vol. 56, no. 4, pp. 1572-1588, Apr. 2008.

[29] A.S. Cacciapuoti, G. Gelli, L. Paura, F. Verde, "Widely-linear versus linear blind multiuser detection with subspace-based channel estimation: finite sample-size effects", *IEEE Trans. Signal Process.*, vol. 57, no. 4, pp. 1426-1443, Apr. 2009.

[30] G. Gelli and F. Verde, "Two-stage interference-resistant adaptive periodically time-varying CMA blind equalization," *IEEE Trans. Signal*

Process., vol. 50, pp. 662–672, Mar. 2002.

[31] A. Ben-Israel and T. N. E. Greville, *Generalized Inverses*. New York: Springer-Verlag, 2002.

[32] D. Darsena, G. Gelli, L. Paura, F. Verde, "A constrained maximum-SINR NBI-resistant receiver for OFDM systems," *IEEE Trans. Signal Process.*, vol. 55, pp. 3032-3047, June 2007.

[33] U. Mengali and A. N. D'Andrea, *Synchronization Techniques for Digital Receivers*. New York: Plenum, 1997.